On the Existence of Cu^{I} Pairs in ZSM-5—A Computational Study

Philipp Spuhler,[a] Max C. Holthausen,*[a] Dana Nachtigallová,[b] Petr Nachtigall,[b] and Joachim Sauer*[c]

Abstract: The siting and coordination of Cu^{I} pairs in zeolite ZSM-5 have been studied by means of a combined quantum mechanics/interatomic potential function technique (QM-Pot). It couples a density functional theory (DFT) description employing a hybrid functional (B3LYP) for copper ions, including their local environment, with a DFT-parameterized shell model ion-pair potential for the periodic ZSM-5 structure. A missing $Cu^{I}-Cu^{I}$ interaction potential term in the force field has been parameterized on the basis of DFT results. Several distinct coordination sites for Cu^{I} pairs have been identified within the ZSM-5 framework. These have been classified as *open*, *nest*, *open-nest*, and *cage* pairs, owing to the shape of their local environment in the crystal. A nest-shaped, bridged eight-membered ring constitutes the most probable site for the existence of Cu^{I} ion pairs. It is energetically favored over all isolated Cu^{I} sites. The excitation and emission energies for the singlet–triplet transition of the Cu^{I} pairs have been studied. Earlier assignment of an emission band at 520 nm to Cu^{I} pairs by others is not supported by our computed results.

Keywords: copper · density functional calculations · ion pairs · QM-Pot calculations · zeolites

Introduction

In the mid-eighties, Iwamoto and co-workers first reported[1] that the Cu-exchanged zeolite ZSM-5 shows a particularly high and steady activity for the direct catalytic conversion of NO into N_2 and O_2 ("deNO_x activity"). The same system is also active for the selective catalytic reduction (SCR) of NO by hydrocarbons in the presence of excess oxygen.[2] Both findings rendered research on this material highly attractive since its potential use as an alternative to contemporary catalytic converter techniques to remove pollutants from exhaust gas is of obvious environmental and hence industrial relevance. Unfortunately, at the present stage the use of Cu-ZSM-5 is limited by its instability under hydrothermal conditions and facile poisoning by sulfur oxides. Numerous academic and industrial research groups have studied properties and reactivity of this and related systems ever since Iwamoto's discovery. Despite many attempts to characterize the active site in Cu-ZSM-5 and to unveil the mechanism by which NO decomposes,[3–6] neither goal has been achieved up to now. A detailed understanding of this catalyst, however, is a prerequisite for its improvement or the de novo design of new materials. In particular, the nature of active sites and the role of pairs of Cu ions therein is still a matter of debate. This is the subject which we address in this study by computational techniques.

The catalyst of interest, ZSM-5, is a high-silica aluminosilicate of MFI structure type. Twelve unique tetrahedral sites (referred to as T sites, T1 to T12) can be distinguished in its orthorhombic all-silica structure.[7] A characteristic feature of this material is the presence of two major channel types formed by ten-membered rings (i.e., rings consisting of 10 T sites), arranged to form a straight ("main") channel and a perpendicular sinusoidal ("zigzag") channel. In ZSM-5, Al atoms can replace some of the framework Si atoms and the Si/Al ratio can be controlled by synthesis. Each Al site introduces one negative charge to the system, which is balanced by extraframework counterions. Commercially available material usually contains H^{+} or Na^{+} ions. Ion exchange with aqueous copper(II) acetate or nitrate solutions and subsequent reduction of Cu^{II} to Cu^{I} [8–10] yields Cu^{I}-ZSM-5 with variable copper loading (commonly given as exchange level, e.l., defined by $2n_{Cu}/n_{Al}$ in percent). As different Cu and

[a] Dr. M. C. Holthausen, Dipl.-Chem. P. Spuhler
Philipps-Universität Marburg, Fachbereich Chemie
Hans-Meerwein-Strasse, 35032 Marburg (Germany)
Fax: (+49) 6421-2825566
E-mail: max.holthausen@chemie.uni-marburg.de

[b] Dr. D. Nachtigallová, Dr. P. Nachtigall
J. Heyrovský Institute of Physical Chemistry and Center for Complex Molecular Systems and Biomolecules
Academy of Sciences of the Czech Republic
Dolejškova 3, 18223 Prague 8 (Czech Republic)

[c] Prof. Dr. J. Sauer
Humboldt-Universität zu Berlin
Institut für Chemie, Arbeitsgruppe Quantenchemie
Unter den Linden 6, 10099 Berlin (Germany)
Fax: (+49) 30-20937136
E-mail: js@chemie.hu-berlin.de

  0947-6539/02/0809-2099 $ 20.00+.50/0

Cu – O species may be obtained by this procedure, model catalysts prepared by gas-phase ion exchange between H-ZSM-5 and $Cu^{I}Cl$ provide a better defined system for studying Cu^{I} sites.[11]

There are four essential experimental findings and interpretations of relevance for the present discussion concerning the nature of the active site: 1) The turnover frequency (TOF: number of NO molecules converted per Cu ion and unit time) of the decomposition reaction increases with the copper exchange level,[12–15] and zeolites exceeding the exchange level of 100 % show a very high catalytic activity. Furthermore, the conversion ratio (that is, twice the amount of N_2 or O_2 produced, divided by the amount of NO utilized) shows an S-shape dependence on the e.l.[16] From these data it has been reasoned that either the active site consists of two or more adjacent Cu ions or there are two or more single Cu ion sites, with the catalytically more active being less favorable for cation exchange; that is, the active site is populated only after saturation of other coordination positions for the copper ions.[16] 2) The TOF increases with the Si/Al ratio for zeolites with an e.l. below 90 %, but decreases with the Si/Al ratio for zeolites with an e.l. above 90 %.[13] This led some authors to propose Cu pairs anchored to next-nearest-neighbor Al sites in the zeolite framework as active site.[12–14] 3) On the basis of EXAFS, IR, and photoluminescence data, Lamberti et al. suggested two different types of sites, characterized by 490 nm and 535 nm bands in the emission photoluminescence spectra and by 256 nm and 300 nm bands in the photoluminescence excitation scan.[11] They explained the differences in the emission and excitation spectra by differences in the first coordination shell, that is by three- and twofold coordinated isolated Cu^{I} species. Nachtigallová and Nachtigall corroborated these interpretations in two subsequent computational studies.[17, 18] Dědeček and Wichterlová also found two dominant bands at 480 nm and 540 nm and observed that the relative intensities of these bands depend on the Si/Al ratio and the Cu concentration.[19] For low Si/Al ratios and low Cu concentrations the 480 nm peak becomes dominant, whereas the 540 nm peak has been observed for high Si/Al ratios and high Cu concentrations. However, these authors came up with a different explanation: they assumed that the former band is due to Cu^{I} ions adjacent to two Al framework atoms and the latter due to Cu^{I} ions in the vicinity of only one Al framework atom.[19] Moreover, they have found that the number of sites that give the 540 nm band correlates with the activity of the zeolite.[15, 20] Anpo et al. observed three bands in the photoluminescence spectrum at 420 nm, 470 nm, and 520 nm of Cu-ZSM-5.[21] The last band and an excitation band at 310 nm were assigned to Cu^{I} dimer species, while the other two were attributed to isolated Cu^{I} species. Here we note in passing that in the ZSM-5 samples investigated by all these groups the number of Cu ions per unit cell was two at most; this fact renders the occurrence of Cu^{I} pairs rather unlikely. 4) EXAFS measurements on Cu-ZSM-5 with various Cu loadings and Si/Al ratios indicate a Cu – O distance in the range between 1.93 and 2.00 Å.[9, 11, 22, 23] The average coordination number of Cu^{I} ions in Cu-ZSM-5 prepared by gas-phase reaction of H-ZSM-5 with CuCl is 2.5.[11] For zeolites pretreated with hydrogen, Cu – Cu distances between 2.95 and 3.00 Å as well as very short Cu – Cu distances in the range of 2.53 – 2.57 Å have been reported.[9, 23, 24] The longer Cu – Cu distances have been attributed to oxygen-bridged Cu pairs, while the closer contacts were interpreted as evidence for the presence of metal clusters.[9]

Until now neither experimental technique applied to metal-ion-exchanged ZSM-5 has led to an unequivocal identification of the local environment of active sites. Owing to the low Cu^{I} ion concentration (the Si/Al ratio is typically greater than 10 for experimentally used material) and the presence of a variety of binding sites with markedly different properties, the direct assessment of structural information is virtually impossible. Therefore all published interpretations based on experimental data—whether favoring or disfavoring the existence of copper ion pairs in Cu-ZSM-5—remain tentative so far.

From a computational point of view, systems like Cu-ZSM-5 constitute severe challenges for a balanced treatment of both the zeolite framework with its large unit cell (96 T sites and 192 oxygen atoms, $20 \times 20 \times 13.5$ Å) on the one hand and the subtle electronic effects present in active sites containing first-row transition metals on the other hand. Both the application of interatomic potential functions applied in a periodic treatment of the zeolite and the use of very small model systems in a quantum chemical approach severely limit predictive capabilities: molecular mechanics (MM or Pot) do not explicitly take any electronic effects of the transition metal center into account, and the choice of a small framework region in a quantum-chemical treatment completely ignores lattice constraints and steric effects as well as long-range electrostatic interactions due to the zeolite framework.[25] The highly desirable full periodic quantum-mechanical treatment of Cu-ZSM-5, even at moderate levels of approximation, is not yet feasible for systems of such size on a routine basis. The only viable approach is provided by embedding methods, which combine quantum mechanics for the active sites with interatomic potential functions for the periodic zeolite structure. The combined quantum mechanics – interatomic potential function approach (QM-Pot)[26, 27] has indeed led to a variety of interesting conclusions for the properties of single copper ion centers in Cu-ZSM-5[17, 18, 28–30] and Cu-FER.[31] In this study we employ the same strategy to investigate the existence of copper ion pairs in Cu-ZSM-5 and their properties. For earlier computational studies concerning Cu ion pairs in zeolites, see refs. [32 – 34].

Computational Methods and Models

The QM-Pot approach: Within the QM-Pot approach,[26, 27] a small model system ("cluster", C) is cut out from the infinite structure of the Cu-ZSM-5 system (S) retaining the atomic positions for the common set of atoms. The model system contains all atoms needed for a correct description of the electronically demanding site (that is, the binding region of the Cu^{I} ions including neighboring atoms of the framework). The energy $E_{QM}(C)$ of this structure is obtained by quantum mechanics. A second calculation for the same model system employs interatomic potential functions to give an energy $E_{Pot}(C)$. The whole periodic zeolite structure itself is described in a third calculation by interatomic potential functions resulting in a single-point energy $E_{Pot}(S)$. All three energies obtained in this way are then combined to $E_{QM\text{-}Pot}(S)$ according to Equation (1).

0947-6539/02/0809-2100 $ 20.00+.50/0 *Chem. Eur. J.* **2002**, *8*, No. 9

$$E_{\text{QM-Pot}}(S) = E_{\text{Pot}}(S) - E_{\text{Pot}}(C) + E_{\text{QM}}(C) \quad (1)$$

This definition of the QM-Pot energy can be understood as follows: In order to correct the low-level energy $E_{\text{Pot}}(S)$ of the whole system for electronic structure effects, the low-level energy of the active site, $E_{\text{Pot}}(C)$, is "cut out" and replaced by a high-level energy $E_{\text{QM}}(C)$. Thus, the term $-E_{\text{Pot}}(C)+E_{\text{QM}}(C)$ can be understood as a quantum-mechanical correction for the electronically demanding site within the zeolite. Equation (1) defines a consistent potential energy hypersurface of the system and allows not only for the calculation of a combined energy, but also for the computation of combined gradients essential for the optimization procedure and a combined Hessian necessary to characterize stationary points. Geometry optimizations are performed on the whole system in cartesian coordinate space. Whenever the definition of the model system requires the breaking of chemical bonds, open valences are saturated by addition of link atoms. In the present study, this concerns only O–Si bonds, which are substituted by O–H bonds in the model system. During geometry optimization the additionally introduced atoms are kept aligned along the original O–Si bonds of the whole system at a fixed distance such that the potential energy surface correctly depends on 3N cartesian degrees of freedom. A detailed description of the choice of the model systems is given below; for further details of the method see ref. [27]. All QM-Pot calculations were carried out with the QMPOT program,[25] which combines energies and gradients obtained with the TURBOMOLE[35] and GULP[36] programs for electronic structure and classical force-field calculations, respectively. Additional calculations (evaluation of analytic second derivatives, NBO analysis) were performed using the Gaussian 98 suite of programs.[37]

Electronic structure calculations: For a description of chemical reactions or an understanding of spectroscopic properties like, say, photoluminescence spectra, correlated levels of electronic structure theory have to be applied. While the application of post-Hartree–Fock methods is limited to small systems, density functional theory (DFT)[38] provides a valuable compromise between accuracy and computational effort. In this study we employ the B3LYP exchange-correlation functional.[39] For the atoms H, Si, Al, and Cu the DZP and for O the TZP basis sets, respectively, were chosen from the TURBOMOLE library,[40] T(O)DZP for short. The contraction scheme is (4s1p) → (2s1p)/[31/1] for H, (11s7p1d) → (6s4p1d)/[521111/4111/1] for Si and Al, (14s10p5d) → (8s6p3d)/[62111111/331111/311] for Cu, and (10s6p1d) → (6s3p1d)/[511111/411/1] for O. Neither relativistic effects nor corrections for the basis set superposition error have been taken into account in this study.

Interatomic potential functions: A shell-model ion-pair potential was used as the classical part in the QM-Pot calculations. In this approach atoms are considered as ions with formal charges corresponding to their valence states (H^+, Si^{4+}, Al^{3+}, O^{2-}, Cu^+) and all atomic interactions are described by analytical functions. These functions contain long- and short-range terms, the former describing Coulomb attraction and repulsion of charges, the latter describing interactions that cannot be assigned to simple electrostatics. The polarizability of the anions (O^{2-} in this case) is taken into account by a shell model, which divides each anion into a negatively charged shell and a positively charged core coupled by a harmonic spring, thereby treating each anion as a flexible dipole.

A detailed description of the shell-model ion-pair potential is given in ref. [41]. The parameters in the functional terms for the interaction between H, Si, Al, and O atoms have been derived by fitting to a DFT description of model systems.[42] In the same way, parameters for the Cu–O interaction have been determined,[17] as well as those for the Cu–Cu interaction, which we present in this study. A standard procedure implemented in the program GULP was used to fit the parameters to DFT gradients of model systems by a least-squares method. The database for parameter fitting included data from a simple D_{2h}-2-T site model for different Cu–Cu distances (see next section) and was extended during the QM-Pot lattice energy minimizations by inclusion of DFT gradients of several model systems obtained in the course of geometry optimizations. The short-range term for the Cu–Cu interaction was chosen to be of Morse type, as described by Equation (2). The adjusted parameters are $D = 1.5748576$ eV, $\alpha = 1.5232$ Å^{-1} and $r_0 = 2.21038$ Å, for a cut-off distance of 10 Å.

$$E(r) = D\{[1 - \exp(-\alpha[r - r_0])]^2 - 1\} \quad (2)$$

This shell-model ion-pair potential has been applied to a unit cell containing 96 T sites (94 Si atoms and 2 Al atoms) using periodic boundary conditions. Lattice energy minimizations have been performed without symmetry constraints ($P1$ symmetry). Cell parameters have been determined for each Al distribution by constant pressure calculations, in other words completely unconstrained optimizations, at the interatomic potential function level by means of GULP. Because a reliable Cu^{I}–Cu^{I} potential was not available at the beginning of our investigation, the determination of the cell parameters was carried out without Cu ions in the unit cell. Subsequently, constant-volume calculations for the unit cell, that is, an optimization with fixed cell parameters with 2 Cu^{I} ions included, have been performed at the interatomic potential function level for a reasonable structure guess. This preoptimized structure was used as an initial estimate for subsequent constant-volume QM-Pot lattice energy minimization by the program QMPOT, in which the atoms were allowed to relax but the cell parameters were fixed.

Selection of model systems: The cluster models were chosen according to the following procedure: 1) All framework O atoms less than 2.5 Å from Cu^{I} ions were considered as first coordination shell and included in the cluster.[17] 2) All T sites (Si or Al atoms at the center of a framework tetrahedron) directly connected to these atoms, as well as the remaining O atoms forming their tetrahedral environment, were included in the cluster. 3) The bonds connecting these tetrahedra to the framework were cut and the resulting open valences were saturated by H atoms. These atoms were kept aligned along the respective "substituted" O–Si bond of the whole system in QM-Pot geometry optimizations and the O–H bond lengths were fixed to 0.9666 Å and 0.9628 Å for Si-O-H and Al-O-H moieties, respectively. 4) If more than one bond to a particular framework tetrahedron was broken, the entire subunit (i.e., T site plus all connected O atoms) was included in the cluster in order to avoid computational artifacts due to close H–H contacts.

Results and Discussion

A first model study: A first indication of the existence of Cu^{I} pairs emerged from a preliminary study of a simple model consisting of two C_{2v}-symmetric [CuAl(OH)$_4$] species, corresponding to a symmetrized representation of one of the most likely coordination sites of a single Cu^{I} ion in ZSM-5, referred to as ***I2*** in previous work.[17] As a simple model we combined two such species to make a D_{2h}-symmetric structure. Our initial aim was to learn about potential deviations from a purely repulsive Coulomb curve resulting from the orbital interaction of two neighboring Cu^{I} centers. However, the quite unexpected result of the relaxed Cu–Cu distance scan in the D_{2h}-[CuAl(OH)$_4$]$_2$ system is shown in Figure 1. The scan reveals a minimum at 2.46 Å, 8.5 kcal mol^{-1} deep with respect to two isolated [CuAl(OH)$_4$] moieties. In order to substantiate our finding, we evaluated the Hessian elements at the minimum structure, optimized within D_{2h} symmetry. An inspection of the harmonic frequencies revealed eleven imaginary modes, all below 220i cm^{-1}, which identifies this structure as a higher order saddle point without any chemical relevance. Subsequent geometry optimizations following each of the imaginary modes "downhill" led to major geometric rearrangements and finally converged on the D_2-symmetric dimer structure depicted in Figure 2. Subsequent evaluation of harmonic frequencies indeed verified this species as a true minimum on the potential energy hypersurface, with a Cu–Cu distance of 2.73 Å. Relative to two isolated C_2-symmetric [CuAl(OH)$_4$] fragments (symmetry has also been relaxed for the fragments in order to dispose three imaginary modes

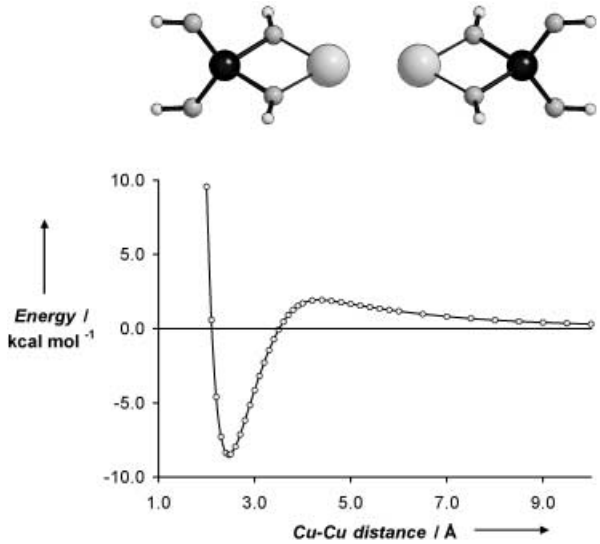

Figure 1. Energy of the D_{2h}-[{CuAl(OH)$_4$}$_2$] model as a function of the Cu – Cu distance, obtained by symmetry-constraint structure optimizations at given Cu – Cu distances. The apparent minimum structure at 2.46 Å is in fact a higher order saddle point on the potential energy surface.

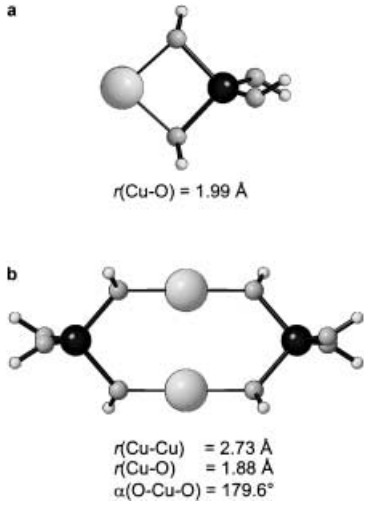

Figure 2. a) Optimized C_2-[CuAl(OH)$_4$] model. b) Optimized D_2-[{CuAl(OH)$_4$}$_2$] model in the electronic ground state (^{1}A).

revealed by harmonic frequency analysis), the dimer is bound by 80 kcal mol^{-1}.

This species bears structural features very different from the D_{2h} starting point of the investigation, but closer inspection of the literature revealed a variety of examples for Cu^I salts with a very similar local coordination environment for the copper ions. In inorganic and organometallic chemistry several examples of multinuclear copper(I) complexes are known that have Cu – Cu contacts comparable to the smallest Cu – Cu distance of 2.56 Å in metallic copper. Some of these exhibit extraordinary closed shell interactions, which have already been subject to theoretical investigation (see references cited in ref. [43]). In particular, bidentate ligands such as acetate, trifluoroacetate, and benzoate have been characterized as multinuclear complexes that share a key structural property with the D_2-symmetrical dimer—a parallel arrangement of linear O-Cu-O units.[44] The strongest similarity is shown by gaseous Cu^I acetate, which is also a dimer.[45] This structural feature is not even limited to oxygen ligands or to Cu^I as a central ion. Cu^I azenido compounds [{Cu^I(RN$_3$R)}$_2$] as well as Au^I dithiocarbamates [{Au(R$_2$NCSS)}$_2$] show equivalent structures.[43] Given the high stability of the D_2 species, we searched for potential positions of such species within the zeolite framework. And in fact, as detailed below, this bonding pattern is the heart of highly reasonable candidates for Cu^I pairs in Cu-ZSM-5.

A referee wondered whether the density functions currently in use are capable of describing these special dispersion-type closed-shell interactions. First, we note that we are not in the region of vanishing density overlap where this problem does indeed become critical. Second, the interaction between the two ***I2***-[CuAl(OH)$_4$] units is rather an effect of 4s/3d hybridization and orbital interactions at both Cu^I fragments (see *Electronic structure of Cu^I pair species*, below), which are both described reasonably well by B3LYP.

Structures of Cu^I pairs in the zeolite: More or less arbitrarily, we consider an arrangement of two Cu^I ions a pair if the Cu – Cu distance is shorter than 3.0 Å—a criterion based on structural, not electronic, properties. The simplest way to investigate copper aggregation is to consider two Cu^I ions per unit cell only. This implies that two of the 96 Si tetrahedral sites of the unit cell are exchanged for Al atoms in order to avoid an overall charge. This situation corresponds to a Si/Al ratio of 47. There are ample possibilities for the distribution of Al and Cu atoms within the ZSM-5 unit cell and a systematic, exhaustive search seems impossible. Previous calculations have shown that Cu^I ions preferentially coordinate to O atoms belonging to AlO$_4$ tetrahedra within the framework,[17] but there are no distinguished crystallographic sites for Al substitution. We therefore started our search for pair sites by generating starting geometries in which Cu^I pairs are located at coordination sites with two neighboring Al positions separated by one, two, or three SiO$_4$ tetrahedra. Figure 3 shows all types of coordination sites for which pair structures resulted from the geometry optimizations.

A selection of the model systems that have been optimized by the QM-Pot approach is shown in Figures 4 – 9. All are described by minimum cluster sizes according to the rules outlined above, except for the open-nest pair (Figure 8). The smallest distance found between two Cu^I ions coordinated at such sites was 2.55 Å (open site, see below), which compares well to the closest metal – metal contact in metallic copper (2.56 Å). We have classified the structures according to their local environment as open pairs (***O***), nest pairs (***N***), open-nest pairs (***ON***), and cage pairs (***C***). Let us now turn to the discussion of the distinct structural features, an overview of which is given in Table 1.

Open pairs: The coordination site of an open pair consists of a five-membered chain of T sites (Figure 4). This site can be regarded as a superposition of two neighboring ***I2*** sites, according to the nomenclature introduced in ref. [17]. All such pairs are located at the intersection of main and sinusoidal channels and, hence, should be accessible to adsorbates from both directions. Cu^I ions at ***O*** sites reach

  0947-6539/02/0809-2102 $ 20.00+.50/0 *Chem. Eur. J.* **2002**, *8*, No. 9

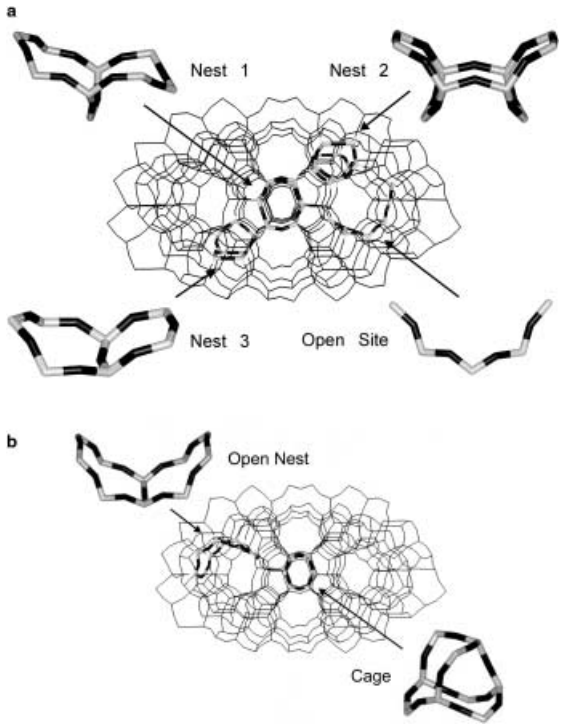

Figure 3. Sketch of the individual types of Cu[I] pair sites and their location within the ZSM-5 framework. View along the main channels, represented by ten-membered rings, perpendicular to the sinusoidal channels. a) The sites denoted as "nest 1–3" are located on the wall of the sinusoidal channel and the "open sites" are on the edge of the sinusoidal and the main channel. b) The "open nest" is located on the wall of the main channel and the "cage" encloses an area that belongs neither to the main nor to the sinusoidal channel. Tetrahedron sites are shaded bright and connecting oxygen atoms dark.

Table 1. Selected structural properties of Cu[I] pairs in Cu-ZSM-5 (bond lengths in Å).

Site[a]	r(Cu–Cu)	r(Cu–O)[b]	CN(O)[c]	CN(O_{Al})[d]
O(2,12/1)	2.70	2.00, 2.07 / 2.01, 2.07	2/2	2/2
O(6,9/1)	2.55	2.03, 2.04 / 2.02, 2.03	2/2	2/2
O(2,5/1)	2.69	2.03, 2.05 / 1.99, 2.08	2/2	2/2
N1(7′,10′/1)	2.63	1.93, 1.95 / 1.98, 2.02[e]	2/2	2/2
N1(1,7/2)	2.82	1.94, 1.99, 2.37 / 1.99, **2.15**, **2.21**	3/3	3/1
N1(4,10/2)	2.61	1.99, 2.01, 2.16 / 2.07, **2.09**, 2.45	3/3	3/2
N1(5,11/2)	2.78	1.92, 1.96 / **2.10**, 2.13, **2.18**	2/3	2/1
N1(7,10′/2)	2.65	1.99, **2.05**, **2.39** / 1.99, 2.03	3/2	1/2
N1(7′,10/2)	2.61	1.99, **2.06**, **2.46** / 1.99, 2.03, 2.20	3/3	1/3
N1(11,11/2)	2.82	1.96, **2.01** / 2.01, **2.07**, 2.26	2/3	1/2
N1(1,7/3)	2.76	1.97, **2.06**, **2.29** / 1.99, **2.15**, **2.36**	3/3	1/1
N1(4,10/3)	2.66	2.02, **2.08**, 2.15 / 2.09, **2.10**, 2.17	3/3	2/2
N2(7,12/2)	2.64	2.09, 2.10, 2.22 / 2.02, 2.16	3/2	3/2
N2(7,12/1)	2.63	2.03, 2.20, **2.28** / 2.04, 2.05	3/2	2/2
N3(9,10/1)	2.56	2.10, 2.19, 2.32 / 2.01, **2.09**, **2.49**	3/3	3/1
C(5,11/2)	2.61	1.98, **2.06** / 2.01, 2.08, **2.26**	2/3	1/2
ON(7,12/2)	2.86	2.03, 2.11 / **2.06**, 2.14, **2.17**	2/3	2/1

[a] For a definition of clusters ***O***, ***N1***, ***N2***, ***N3***, ***C***, ***ON*** see Figures 4–9. Numbers before the slash indicate the T sites substituted by Al atoms. The classification is based on the orthorhombic structure of high-silica ZSM-5. The number following the slash refers to the number of Si sites separating the Al sites. [b] Distance to oxygen atoms closer than 2.50 Å. **Bold** numbers refer to oxygen atoms not bound to Al atoms. The numbers before and after the slash relate to the Al site given first and second in the pair classification, respectively. [c] Number of oxygen atoms with Cu–O distances less than 2.50 Å. The numbers before and after the slash relate to the Al site given first and second in the pair classification, respectively. [d] Number of oxygen atoms bound to Al atoms with Cu–O distances less than 2.50 Å. The numbers before and after the slash relate to the Al site given first and second in the pair classification, respectively. [e] Both Cu[I] ions are closer to Al at T7′.

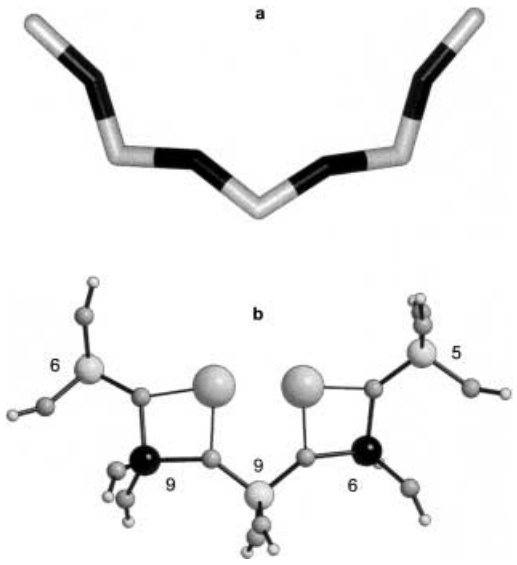

Figure 4. a) Open site for Cu[I] pairs including the nearest Si/Al sites (bright/black) and the connecting oxygen atoms (dark). b) Model system of the ***O***(6,9/1) pair. Numbers denote the T sites in the orthorhombic ZSM-5 structure.

into an "open space" within the ZSM-5 structure and the oxygen coordination number is rather small, two per Cu[I]. The particular coordination mode (each copper coordinates to one T site only) introduces some flexibility into the position of both Cu[I] ions, and framework O atoms available for coordination in the closer environment easily lead to a separation of both ions. Consequently, only three different open pairs could be located, whereas many structures initially created as ***O***-pairs collapsed into two isolated sites in the course of geometry optimization. We designate the remaining pairs as ***O***(2,12/1), ***O***(2,5/1), and ***O***(6,9/1). Numbers before the slash denote the T sites substituted by Al atoms, on the basis of their classification in the orthorhombic structure of the all-silica ZSM-5,[7] while the number following the slash denotes the smallest number of Si sites separating the two Al sites. As mentioned already, the Cu–Cu distance in ***O***(6,9/1), 2.55 Å, is the smallest found in this study.

Nest pairs: In structural terms, nest pairs (***N*** sites) differ greatly from ***O*** sites. In these species each Cu[I] ion is bound to oxygen atoms such that the local ion arrangement is much less flexible than in open pairs. We found three different ***N*** sites (see Figures 5–7), all located at walls of the sinusoidal channel, and thus easily accessible for adsorbates. Overall, for ***N*** species the oxygen coordination numbers are two or three, and all nests identified consist of a combination of four-, five-, or six-membered rings forming larger seven- or eight-membered rings. Despite careful searches, we were unable to locate Cu[I] pairs coordinated to just one five- or six-membered ring, either in the main or in the sinusoidal channel. Apparently, ring sizes smaller than seven do not lead to stable Cu[I] pairs.

Nest 1 consists of an eight-membered ring bridged by one T site (Figure 5). This type of site can be regarded as a superposition of two six-membered rings which have been identified as very stable coordination sites for isolated copper ions in former work, designated ***Z6*** sites.[17] The oxygen

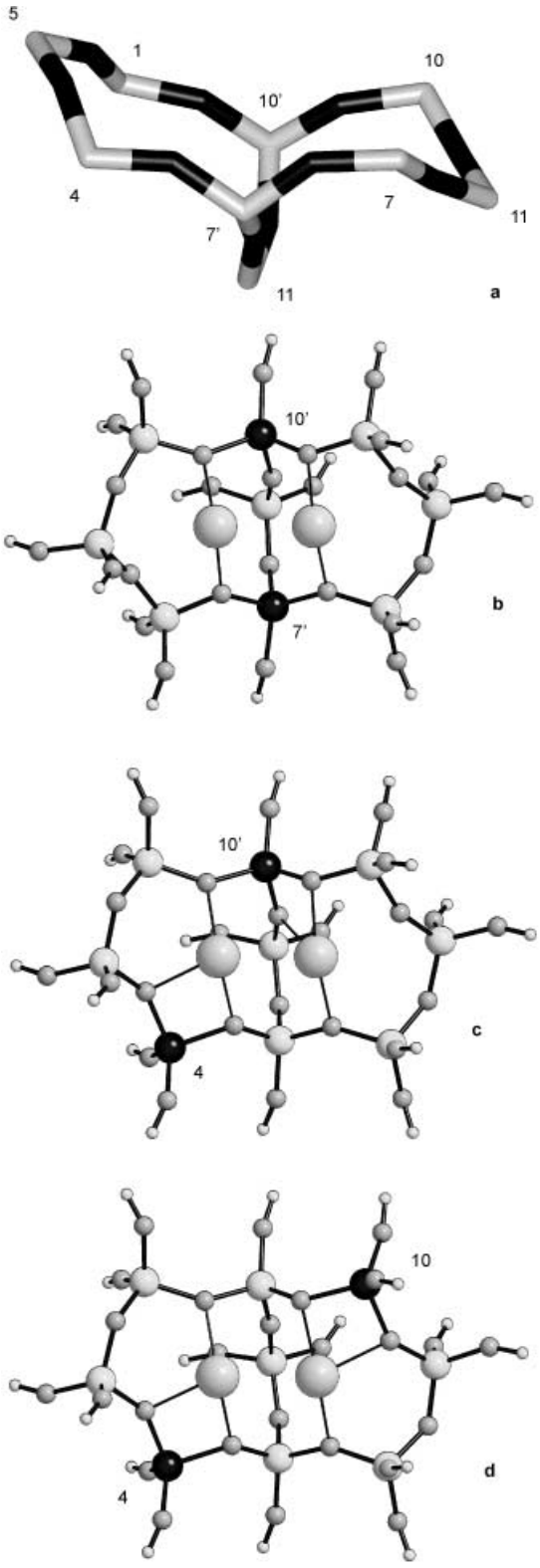

Figure 5. a) Nest 1 for Cu^I pairs. b) Model system of the ***N1***(7′,10′/1) pair. c) Model system of the ***N1***(4,10/2) pair. d) Model system of the ***N1***(4,10/3) pair.

coordination number per Cu^I ion ranges from two to three, depending on the particular binding situation (see below). Remarkably, Cu^I pairs occur for nine out of ten Al distributions investigated within the nest. Between one and three SiO_4 tetrahedra can separate Al sites without preventing the formation of Cu^I pairs. Only in one case, namely ***N1***(5,11/3), is the Cu – Cu distance greater than 3 Å (3.16 Å). The D_2-$[Cu_2\{Al(OH)_4\}_2]$ gas-phase model and the ***N1***(7′,10′/1) pair show very similar structural features (since the previous nomenclature is not unequivocal, in this case we had to distinguish between two T7 and two T10 sites—see Figure 5). In both structures each copper ion is almost linearly coordinated to two oxygen atoms with Cu – Cu distances of 2.73 and 2.63 Å, respectively. Evidently, in line with our findings for the D_2-$[Cu_2\{Al(OH)_4\}_2]$ system, this particular orientation of two $Al(OH)_4$ tetrahedrons provides an optimal coordination environment for the Cu^I pair. Similar bonding patterns are visible in most of the ***N1*** sites.

N2 sites also consist of an eight-membered ring (see Figure 6). Unlike ***N1***, however, the ring is bridged by two Si sites, so the entire binding site consists of two ***Z5*** sites[17] joined by two oxygen bridges. In all ***N2***-pairs found, the Al sites are separated by one or two SiO_4 tetrahedra. The oxygen coordination number is different for the two copper ions (2

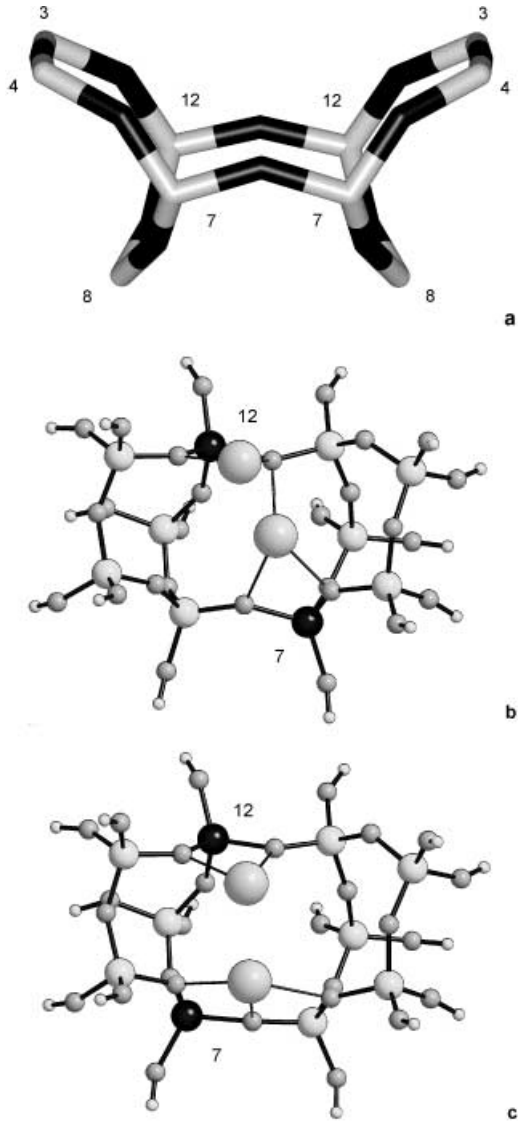

Figure 6. a) Nest 2 for Cu^I pairs. b) Model system of the ***N2***(7,12/2) pair. c) Model system of the ***N2***(7,12/1) pair.

  0947-6539/02/0809-2104 $ 20.00+.50/0 *Chem. Eur. J.* **2002**, *8*, No. 9

and 3, respectively) and, as shown in Figure 6, one of the ring oxygen atoms coordinates both ions in case of the ***N2***(7,12/2) pair. Figure 6 also shows that the coordination mode of copper in the vicinity of the aluminum atom at the T12 position resembles the binding mode of an ***I2*** site for the monomer.

We found a third type of nest structures, denoted as ***N3***, consisting of a seven-membered ring (see Figure 7). It can be regarded as a combination of a ***Z5*** and a ***Z4*** site,[17] and the

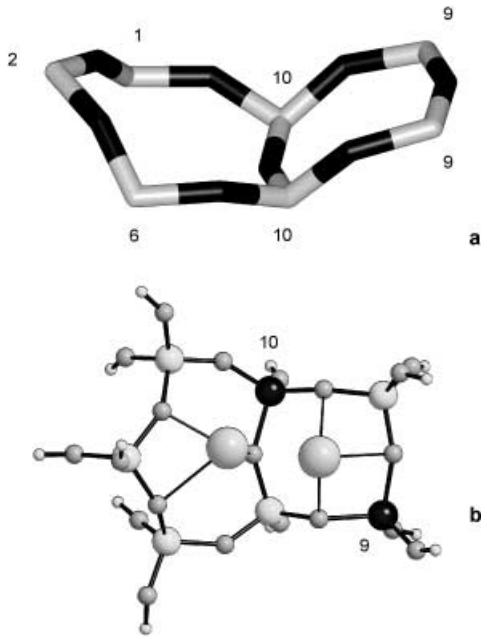

Figure 7. a) Nest 3 for Cu[I] pairs. b) Model system of the ***N3***(9,10/1) pair.

oxygen coordination number is three per Cu[I] ion. This pair type only exists for an arrangement of two Al sites separated by one Si site as a stable minimum structure with a very short Cu–Cu distance of 2.56 Å.

Open-nest pairs: As noted above, it was impossible to locate pairs solely coordinated to one five- or six-membered ring. Instead, nests in the main channel consist of a combination of such rings (designated ***M5*** and ***M6*** sites in ref. [17]). These combinations lead to rather flat structural moieties (compared with the possible combinations of rings within the sinusoidal channel) to which we refer as open nests (***ON***). We were able to locate one pair of this type, which is shown in Figure 8. The structure contains one copper center bound to three oxygen atoms of a ring (corresponding to the ***M6*** site) while the other is bound to two oxygen atoms of a single tetrahedron site only (corresponding to an ***I2*** site). Two Si sites separate the Al sites. The Cu–Cu distance of 2.86 Å is larger than in all other pair structures identified. In fact, this species is unstable with respect to a cluster in which the two copper ions are separated by 3.98 Å (Figure 8). In this competing structure, both ions are coordinated to ***M6*** sites. As the cluster size and connectivity is identical for both species, we can directly compare total QM-Pot energies: the energy difference of 22 kcal mol^{-1} in favor of the latter renders the existence of this pair highly unlikely.

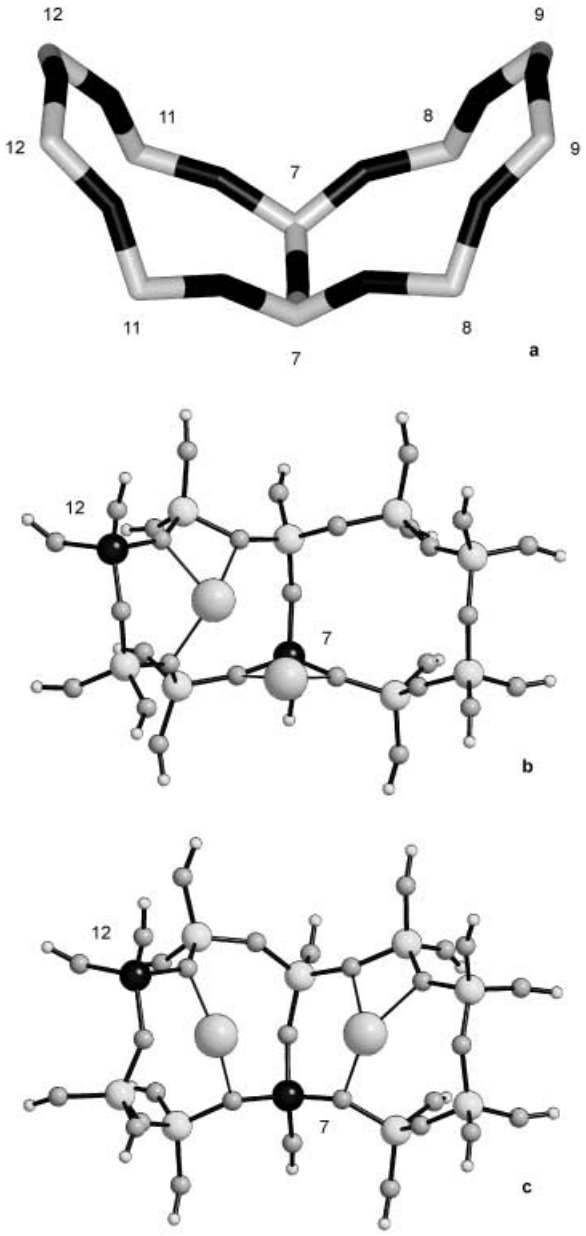

Figure 8. a) Open nest for Cu[I] pairs. b) Model system of the ***ON***(7,12/2) pair. c) Model system with separated Cu[I] ions.

Cage pairs: Another rather stable pair species in which the Cu[I] ions are surrounded by oxygen atoms was classified as cage-type (***C***) (Figure 9). The Al sites are separated by 2 SiO_4 tetrahedra in this structure. The oxygen coordination numbers for the two copper ions are two and three. The twofold coordinated Cu[I] reaches out of the cage formed by nine T sites and into the sinusoidal channel. However, most of the local environment of the ***C***-pair belongs neither to the main nor to the sinusoidal channel. Correspondingly, we expect that this area is less accessible for adsorbates than all other pair sites we found.

In summary, the Cu–Cu distances for all types of pairs fall into the range between 2.5 and 2.9 Å. The larger distances come very close to the Cu–Cu distances usually assigned to Cu-(O)-Cu species in experimental work, whereas smaller distances are very similar to the Cu–Cu distance ascribed to

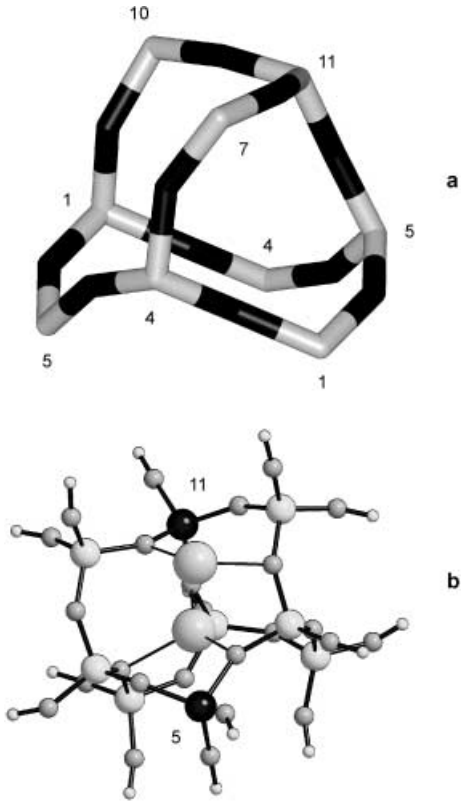

Figure 9. a) Cage for Cu^{I} pairs. b) Model system of the ***C***(5,11/2) pair.

Cu^0-Cu^0 bonds in metal clusters.[9] The Cu–O distances for the first coordination shell and the average oxygen coordination number between two and three do not differ from the values predicted previously for isolated Cu^{I} binding sites.[17] Hence, it will not be possible to identify $Cu^{I}-Cu^{I}$ pairs in zeolites from this data.

Dissociation energies and relative energies: When discussing energies we have to keep in mind that a direct comparison of QM-Pot energies obtained according to Equation (1) is meaningful only for model systems with identical size and connectivity to the zeolite framework. That is, we cannot directly compare total energies of different pair sites. We can, however, compare energies for a stepwise dissociation of the two Cu ions if we define the first and total dissociation energies by the Equations (3) and (4).

$$Cu_2Z \rightarrow CuZ^- + Cu^+ \qquad E_{D,first} = E(CuZ^-) + E(Cu^+) - E(Cu_2Z) \qquad (3)$$

$$Cu_2Z \rightarrow Z^{2-} + 2\,Cu^+ \qquad E_{D,tot} = E(Z^{2-}) + 2E(Cu^+) - E(Cu_2Z) \qquad (4)$$

The energy $E_{D,first}$ describes the dissociation energy of one of the copper ions (see below)—for nonsymmetrical clusters this results in two different values, depending on the choice of the ion removed first. $E_{D,first}$ and $E_{D,tot}$ are adiabatic dissociation energies which involve lattice energy minimization for the ZCu^- and Z^{2-} species. Due to the periodic boundary conditions these dissociation energies refer to processes in which Cu^{I} ions are removed from *every* unit cell of the periodic, infinite lattice. In the GULP calculations we added one or two positive background charges, respectively, to every unit cell because otherwise the periodic treatment of the crystal would lead to an infinite number of negative charges. The model systems were treated with the correct charge (for details see ref. [46]).

Table 2 shows a selection of total dissociation energies $E_{D,tot}$ computed according to Equation (4). The data clearly show

Table 2. Dissociation energies of copper pairs according to Equation (4).

Site	$E_{D,tot}$ [kcal mol^{-1}]
O(2,12/1)	297.4
O(6,9/1)	295.3
O(2,5/1)	292.9
N1(7′,10′/1)	319.5
N1(1,7/2)	308.1
N1(4,10/2)	312.0
N2(7,12/2)	294.6
N2(7,12/1)	296.6
N3(9,10/1)	290.4
C(5,11/2)	300.2
ON(7,12/2)	282.2

that two Cu^{I} ions are most strongly bound at ***N1*** sites (312–320 kcal mol^{-1}). The highest total dissociation energy is given for the ***N1***(7′,10′/1) site, which is the site that resembles the local oxygen coordination environment of the optimized D_2-$[Cu_2\{Al(OH)_4\}_2]$ gas-phase model most closely. The dissociation energies for all other sites range from 300 kcal mol^{-1} for ***C***(5,11/2) to 282 kcal mol^{-1} for ***ON***(7,12/2). There is no obvious correlation between $E_{D,tot}$ and the coordination number of copper ions (cf. Tables 1 and 2).

The relative stability of pairs is influenced in part by the stability of the corresponding Al distribution within the zeolite. For an estimate of this effect we computed lattice energies (shell-model potential only) for structures containing the negatively charged Al sites without any charge-compensating counterions $E_{rel,Pot}(Z^{2-})$. At this level, the stabilities of the Al distributions within the various pair sites differ significantly by up to 19 kcal mol^{-1} (Table 3). In agreement

Table 3. Relative energies of ZSM-5 for different Al distributions without copper ions, obtained by the interatomic potential function approach and QM-Pot calculations. The values given in square brackets refer to relative energies within sites of one type.

Classification	$E_{rel,Pot}(Z^{2-})$ [kcal mol^{-1}]	$E_{rel,QM\text{-}Pot}(Z^{2-})$ [kcal mol^{-1}]
O(2,12/1)	19.1 [7.1]	7.2
O(6,9/1)	12.4 [0.4]	0.5
O(2,5/1)	12.0 [0.0][a]	(0.0)[a]
N1(7′,10′/1)	10.3 [4.8]	4.3
N1(1,7/2)	5.5 [0.0][a]	(0.0)[a]
N1(4,10/2)	7.7 [2.2]	0.1
N1(5,11/2)	7.0	
N1(7,10′/2)	5.2	
N1(7′,10/2)	6.2	
N1(11,11/2)	8.0	
N1(1,7/3)	(0.0)[a]	
N1(4,10/3)	4.6	
N2(7,12/2)	7.9 [0.0][a]	(0.0)[a]
N2(7,12/1)	12.8 [4.9]	3.8
N3(9,10/1)	16.7	
C(5,11/2)	7.0	
ON(7,12/2)	6.1	

[a] Arbitrarily set to zero.

  0947-6539/02/0809-2106 $ 20.00+.50/0 *Chem. Eur. J.* **2002**, *8*, No. 9

with Dempsey's rule[47] the relative energies decrease with an increasing number of Si sites between the two Al sites. Hence, structures with AlO_4 tetrahedra separated by just one SiO_4 tetrahedron (***O*** and ***N3*** sites, as well as the ***N1***(7′,10′/1) and the ***N2***(7,12/1) site) are disfavored relative to those separated by two or three SiO_4 tetrahedra. For sites of one type and the same QM part, the relative energies obtained by the shell-model potential alone can be compared with results of QM-Pot calculations. For the selected cases given, Table 3 shows agreement within 2 kcal mol^{-1}. It is known that relative stabilities of different Al distributions are influenced by charge-compensating cations. For example, calculations by Schröder and Sauer for faujasite have shown that if protons were used for charge compensation, the Al atoms preferentially occupy two next-nearest-neighbor positions (Al-O-Si-O-Al).[48] Moreover, in calculations on ZSM-5 with protons as charge-compensating counterions, no preference was found for separation of the Al pairs by two instead of one SiO_4 tetrahedron.[28] Hence, Dempsey's rule cannot serve as an a priori guide for the design of reasonable models for theoretical studies on copper-loaded species within a zeolite system. Correspondingly, a comparison of relative QM-Pot energies for the various families of copper-ion-loaded pair sites (Table 4) reveals the high stability of the ***N1***(7′,10′/1) pair,

Table 4. Relative QM-Pot energies of pairs in Cu-ZSM-5.

Classification	$E_{rel,QM\text{-}Pot}(Cu_2Z)$ [kcal mol^{-1}]
O(2,12/1)	4.7
O(6,9/1)	(0.0)[a]
O(2,5/1)	2.0
N1(7′,10′/1)	(0.0)[a]
N1(1,7/2)	7.1
N1(4,10/2)	3.2
N1(5,11/2)	12.4
N1(7,10′/2)	6.2
N1(7′,10/2)	5.9
N1(11,11/2)	15.1
N1(1,7/3)	14.8
N1(4,10/3)	9.3
N2(7,12/2)	(0.0)[a]
N2(7,12/1)	1.8

[a] Arbitrarily set to zero.

irrespective of the fact that the Al sites are separated by one Si site only.

Because we cannot directly calculate relative QM-Pot energies for systems with different model systems in the quantum part we consider three hypothetical reaction steps and the corresponding energy contributions defined in Equations (4)–(6).

$$Cu_2Z \rightarrow Z^{2-} + 2Cu^{+} \qquad E_{D,tot} = E(Z^{2-}) + 2E(Cu^{+}) - E(Cu_2Z) \qquad (4)$$

$$Z^{2-} \rightarrow Z'^{2-} \qquad E(Z'^{2-}) - E(Z^{2-}) \qquad (5)$$

$$2Cu^{+} + Z'^{2-} \rightarrow Cu_2Z' \qquad -E_{D,tot}(Cu_2Z') \qquad (6)$$

This scheme describes a process in which Cu^{I} ions are removed from the original lattice [Eq. (4)] and Al atoms are moved to different positions to generate a new lattice [Eq. (5)], to which the Cu^{I} ions are subsequently added [Eq. (6)]. While QM-Pot energies are available for reactions (4) and (6), that for step (5) is available only at the potential function level for QM-Pot-optimized structures. Hence, energy differences between sites of different type can be approximated by Equation (7).

$$\Delta E = E_{D,tot}(Cu_2Z) + E_{Pot//QM\text{-}Pot}(Z'^{2-}) - E_{Pot//QM\text{-}Pot}(Z^{2-}) - E_{D,tot}(Cu_2Z') \qquad (7)$$

Table 5 shows these energy differences computed for a variety of pairs relative to one pair structure, denoted as E_{rel}, together with the corresponding energy contributions

Table 5. Relative energies of pairs evaluated according to Equation (7) and Pot lattice energies employing QM-Pot-optimized structures.

Classification	E_{rel}	$E_{rel,Pot//QM\text{-}Pot}$ (Z^{2-}) [kcal mol^{-1}]
O(2,12/1)	27.7	10.2
O(6,9/1)	22.8	3.7
O(2,5/1)	24.9	3.4
N1(7′,10′/1)	(0.0)[a]	4.6
N1(1,7/2)	6.8	0.5
N1(4,10/2)	3.9	1.5
N2(7,12/2)	21.5	1.8
N2(7,12/1)	25.5	7.8
N3(9,10/1)	32.5	8.5
C(5,11/2)	18.0	3.9
ON(7,12/2)	32.2	(0.0)[a]

[a] Arbitrarily set to zero.

$E_{Pot//QM\text{-}Pot}(Z^{2-})$ relative to one particular Al distribution, thus denoted as $E_{rel,Pot//QM\text{-}Pot}(Z^{2-})$. We note a pleasingly small maximum deviation of 2 kcal mol^{-1} (for ***N1***(7,12/1) and ***N2***(7,12/2)) if we compare relative stabilities of species within their respective classes directly obtained as QM-Pot energies (Table 4) and approximated by Equation (7) (Table 5). This may serve as a validation of the approximation defined by Equation (7). The compilation of relative energies reveals a particularly high stability of ***N1***-type pairs with ***N1***(7′,10′/1) as the most stable species among all pair sites investigated. As a remnant of Dempsey's rule for the cation-free framework, $E_{rel,Pot//QM\text{-}Pot}(Z^{2-})$ of ***N1***(7′,10′/1) is slightly higher than that of many other species; however, this is evidently compensated by the large dissociation energy of the two Cu^{I} ions (Table 2).

Relative stabilities of copper ion pairs versus monomers: To compare the stability of Cu^{I} ion pairs with that of monomers, we define an average binding energy per Cu^{I} ion in the pair [Eq. (8)], where $E_{D,tot}$ is defined by Equation (4). Values of E_{av} computed from Table 2 fall into the range between 141 and 160 kcal mol^{-1}, slightly higher than the range of dissociation energies of Cu^{I} monomers obtained by Nachtigallová et al. for a variety of binding sites, which is 138–152 kcal mol^{-1}.[17] In terms of E_{av} we find three nest pair structures, ***N1***(7′,10′/1), ***N1***(1,7/2), and ***N1***(4,10/2), more stable than the most favorable monomer site (***Z6***). An intrinsic shortcoming of this approach, however, is caused by the fact that the dissociation energies $E_{D,tot}$ contain a contribution from the Z^{2-} species in Equation (4). The inherent instability due to Coulomb

repulsion in these doubly charged anions increases the E_{av} value computed for a pair, although this artificial situation is not present in the real zeolite. Rather, we consider a process described in Equation (9).

$$E_{av} = E_{D,tot}/2 \quad (8)$$

$$Cu^1Cu^2Z(Al^1,Al^2) + [Z(Al^1,Si^2)]^- \rightarrow [Cu^2Z(Al^1,Al^2)]^- + Cu^1Z(Al^1,Si^2) \quad (9)$$

In Equation (9), $[Z(Al^1,Al^2)]^{2-}$ stands for the zeolite framework with two negative charges per unit cell with the specific Al positions Al^1 and Al^2, and Cu^1 and Cu^2 being the copper ions closer to the corresponding Al atoms. The process in Equation (9) can be formally divided into two steps, represented in Equations (10) and (11). The first step corresponds to the dissociation of one Cu^I ion from each unit cell, and the energy $E_{D,first}$ connected with this process corresponds to the definition given above in Equation (3). The copper ion is transferred in the second step to an equivalent coordination site in which the Al^2 position has been exchanged by a Si atom (that is, creating a monomer copper site within a zeolite containing one Al atom per unit cell). The transfer energy E_{trans} resulting for the hypothetical overall reaction in Equation (9) is given by Equation (12).

$$Cu^1Cu^2Z(Al^1,Al^2) \rightarrow Cu^+ + [Z(Al^1,Al^2)Cu^2]^- \quad E_{D,first} \quad (10)$$

$$Cu^+ + [Z(Al^1,Si^2)]^- \rightarrow Cu^1Z(Al^1,Si^2) \quad -E_{D,mono} \quad (11)$$

$$E_{trans} = E_{D,first} - E_{D,mono} \quad (12)$$

This approach does not consider compensating cations either, but the effects of charged unit cells are present equally on both sides of the reaction and should be well balanced in terms of E_{trans}. A general comparison of $E_{D,first}$ computed for pair sites (ranging from 121 to 158 kcal mol^{-1}, see Table 6) with dissociation energies $E_{D,mono}$ of monomer sites (138 to 152 kcal mol^{-1}) published previously[17] shows no general preference for either binding situation. A direct comparison can be made for selected cases, in which our pair models contain the monomer site referred to in ref. [17] (Table 6). Among those, we find the monomer copper sites favored except in the case of the ***N1***(7′,10′/1) site, which gives an E_{trans} of -5 kcal mol^{-1}.

For our next approach, we designed a model system that contains both the ***N1***(7′,10′/1) site as well as one monomer site of ***M7*** type,[17] which consists of a six-membered ring (2-1-5-11-7-8) bridged by one T site (T4) (see Figure 10). Model systems of this size cannot be adopted on a routine basis, but for this exemplary case we accepted the computational expenses in order to establish directly the relative stability of pair vs. monomer copper ion sites. If we transfer one copper ion from one of the pair positions to this site, the QM-Pot total energies can be compared directly. Prior to the actual QM-Pot calculations, we explored the relative stability of different Cu^I distributions for aluminum at T7 and T10 at the potential function level. One of the two Cu^I ions in ***N1*** was transferred to various positions within the same unit cell keeping it in contact with one AlO_4 tetrahedron in all cases. The other Cu^I ion was left in its position above either the symmetrical or the unsymmetrical ring. Subsequent geometry optimizations at the interatomic potential function level revealed the two most stable structures depicted in Figure 10b and 10c. After geometry optimization at the QM-Pot level, the transfer of Cu(sym) or Cu(asym) from its position in ***N1*** to ***M7*** causes an increase in energy by 14 and 10 kcal mol^{-1}, respectively. We also optimized the corresponding monomer structures (cf. Figure 10d–e) with the aluminum atom located at T7 and found them nearly identical in energy. Both isolated pair positions—Cu(sym) and Cu(asym)—collapsed into a single structure (Figure 10d) owing to the lack of a second AlO_4 tetrahedron able to afford the highly favorable linear coordination around the copper centers.

Finally, we chose yet another approach to evaluate the relative stability of copper ions bound to the most stable Cu^I monomer and pair sites, ***Z6*** and ***N1***(7′,10′/1), respectively. In a super-cell approach including two Cu^I ions, one proton, and three Al sites embedded in the respective minimum cluster environment, both sites were treated simultaneously in a common quantum part. Specifically, as quantum part in a first unit cell we selected the ***Z6*** monomer site consisting of the T sites 4-5-1-10-11-7, with aluminum at T4.[17] As the quantum part in a second unit cell (generated adjacent to the first by duplication of the cell parameters in the *c* direction) we selected the energetically most favorable Cu^I pair site, ***N1***(7′,10′/1), for which ***Z6*** actually forms the unsymmetrical ring. This super cell was treated periodically in the shell-model ion-pair potential calculations. In this way, we were able to assess directly the energetic consequences of the transfer of one copper ion from a pair site to the monomer site (compensating for the charge of the corresponding vacant binding

Table 6. Dissociation and transfer energies according to Equations (10)–(12).

Classification	$E_{D,first}$[a]	$E_{D,mono}$[b]	E_{trans}
O(2,12/1)	T2: 144.9 / T12 144.7	T12 (***I2***): 148.6	T12: 3.9
O(6,9/1)	T6: 136.7 / T9: 142.7	T6 (***I2***): 148.3	T6: 11.6
O(2,5/1)	T2: 136.1 / T5: 142.7		
N1(7′,10′/1)[c]	Sym: 154.3 / Asym: 155.8	T10′(sym) (***Z6***): 149.0	T10′(sym): -5.3
N1(1,7/2)	T1: 157.6 / T7: 141.5		
N1(4,10/2)	T4: 149.8 / T10: 144.5	T4 (***Z6***): 151.9 / T10 (***Z6***): 149.0	T4: 2.1 / T10: 4.5
N2(7,12/2)	T7: 147.9 / T12: 132.5		
N2(7,12/1)	T7: 131.9 / T12: 135.0		
N3(9,10/1)	T9: 141.6 / T10: 137.2		
C(5,11/2)	T5: 131.5 / T11: 131.5		
ON(7,12/2)	T7: 121.3 / T12: 133.1	T12 (***M6***): 147.6	T12: 14.5

[a] First dissociation energy of single Cu^I ions from a pair according to Equation (10). Reference is given with respect to the Al position from which ions were removed. [b] Data taken from ref. [17]. [c] In the ***N1***(7′,10′/1) pair, both Cu ions are marginally closer to the Al atom at T7 and our nomenclature distinguishing the Cu ion binding sites is no longer unique. We therefore characterize the ions as Cu(sym), which is centered above the symmetric six-membered ring (10-10-11-7-7-11), and Cu(asym), which is centered above the asymmetric six-membered ring (10-11-7-4-5-1).

0947-6539/02/0809-2108 $ 20.00+.50/0 *Chem. Eur. J.* **2002**, *8*, No. 9

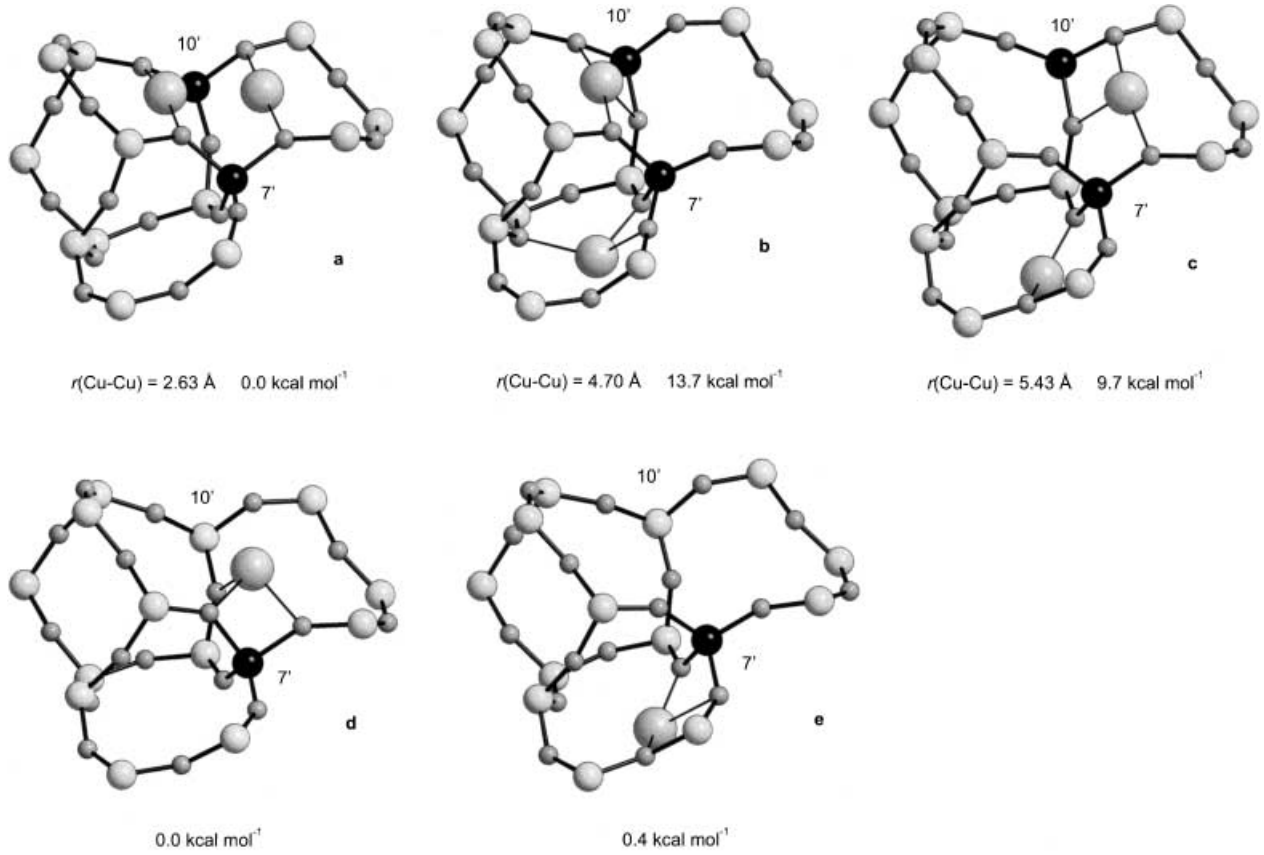

Figure 10. a) Large model system of the ***N1***(7′,10′/1) pair. b) Model system for Al at T7′ and T10′ with separated Cu[I] ions coordinated at the M7 site and the asymmetrical ring of nest 1, or c) the symmetrical ring of nest 1. Energies given are relative to the pair. d) Large model system of Cu[I] monomers for Al at T7′ with Cu[I] coordinated at nest 1 or e) at the M7 site. Energies given are relative to the nest 1 monomer. OH groups are not shown for the sake of clarity.

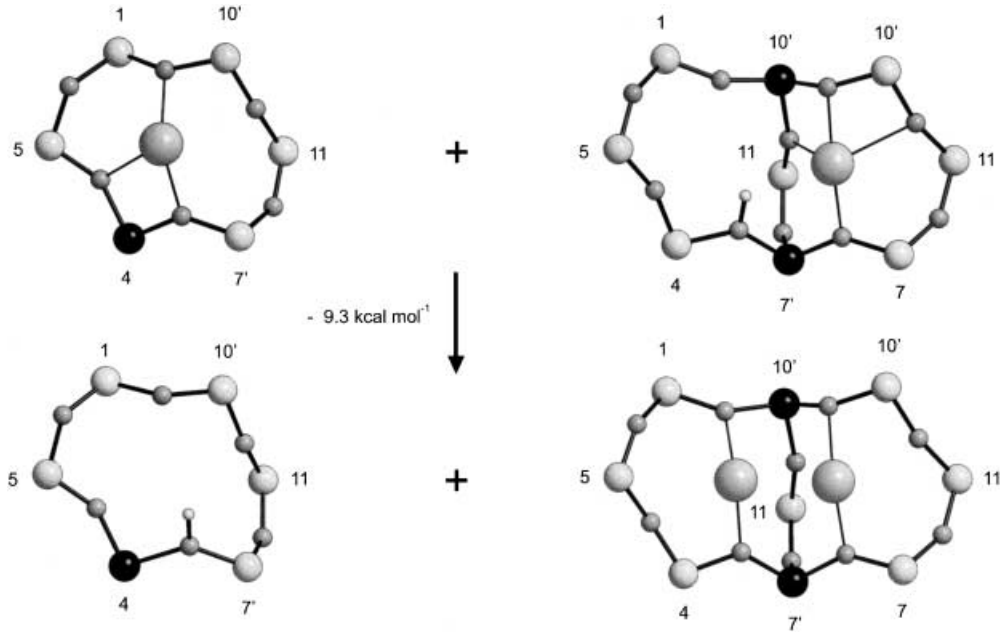

Figure 11. Cu^{I}/H^{+} exchange reaction between the ***Z6*** and the ***N1*** site. OH groups are not shown for the sake of clarity.

site by adding a proton to the coordinating oxygen atoms; see Figure 11) by comparison of total QM-Pot energies. In pleasing agreement with the results obtained above, this approach revealed that the Cu[I] pair is favored by 9 kcal mol^{-1} over the two monomers.

Electronic structure of Cu[I] pair species, excitation and emission spectra: For a qualitative prediction of spectroscopic properties of the various Cu[I] ion pairs, we computed the vertical $T_1 \leftarrow S_0$ excitation and $S_0 \leftarrow T_1$ emission energies as energy difference between triplet and singlet state energies at

singlet and triplet optimized geometries, respectively. The latter can be compared directly with photoluminescence spectra, whereas the former correspond to excitation spectra assuming a spin-forbidden excitation into the lowest triplet state. Experimentally, excitation into the first excited singlet state is observed and thus our calculations will give excitation energies inherently lower than experimental data. Furthermore, our approach neglects vibrational energy corrections and the respective Franck – Condon factors between distinct vibrational levels.

Before we present results for embedded calculations, we shall start our discussion with the electronic structure of the D_2-[{CuAl(OH)$_4$}$_2$] model. In its singlet state (^{1}A) the HOMO and LUMO are of b_3 and a symmetry (Figure 12). The HOMO is an antibonding combination of 3d and 4s hybrid orbitals on each of the copper ions. This hybridization results in efficient polarization of charge density out of the formerly doubly occupied d orbitals away from the O-Cu-O bond axes. This is a common binding mechanism[38] for late transition metal ions, increasing the ability of metal centers without vacant d acceptor orbitals to receive electron density from the donor orbitals (oxygen lone pairs in our case). The LUMO, in turn, is composed of a bonding linear combination of the respective 3d and 4s hybrid orbitals. HOMO and LUMO form the SOMOs in the first excited state ^{3}B$_3$ and therefore the occupation of the former LUMO leads to a significant shortening of the Cu – Cu distance by 0.36 Å and a reduction of the O-Cu-O angle from 179.6° to 163.4°.

In line with this bonding picture, the natural bond orbital (NBO) analysis of the singlet electron density reveals a 4s occupation of 0.48 e$^-$ and a 3d occupation of 9.73 e$^-$ for each of the copper atoms. In the triplet state ($3d^{9.45}4s^{0.72}$) the 4s population is increased by 0.24 e$^-$ and the occupation of the 3d shell is decreased by approximately the same amount (0.28 e$^-$), that is, overall half an electron is transferred from the 3d to the 4s orbitals upon excitation (Table 7).

Figure 13 shows the character of frontier orbitals for the QM part of the ***O***(6,9/1) pair: the SOMO-1 and SOMO for this open site in the triplet state correspond to the HOMO-1 and the LUMO in the singlet state. The SOMO-1 comprises 3d – 4s atomic hybrid orbitals on each of the copper centers

Table 7. Results of NBO analysis for the D_2-[{CuAl(OH)$_4$}$_2$] model system with RB3LYP and ROB3LYP, respectively.

	Natural charges			Natural population				
Atom	Singlet	Triplet	Orbital	Singlet	Triplet total	Triplet α	Triplet β	Spin density[a]
Cu	+0.77	+0.78	4s	0.48	0.72	0.50	0.23	0.85
			3d	9.73	9.45	4.98	4.47	
O[b]	−1.24	−1.23	2s	1.78	1.80	0.91	0.89	0.06
			2p	5.44	5.42	2.74	2.68	
Al	+2.12	+2.12						

[a] Mulliken analysis. [b] Oxygen atoms next to the copper atoms.

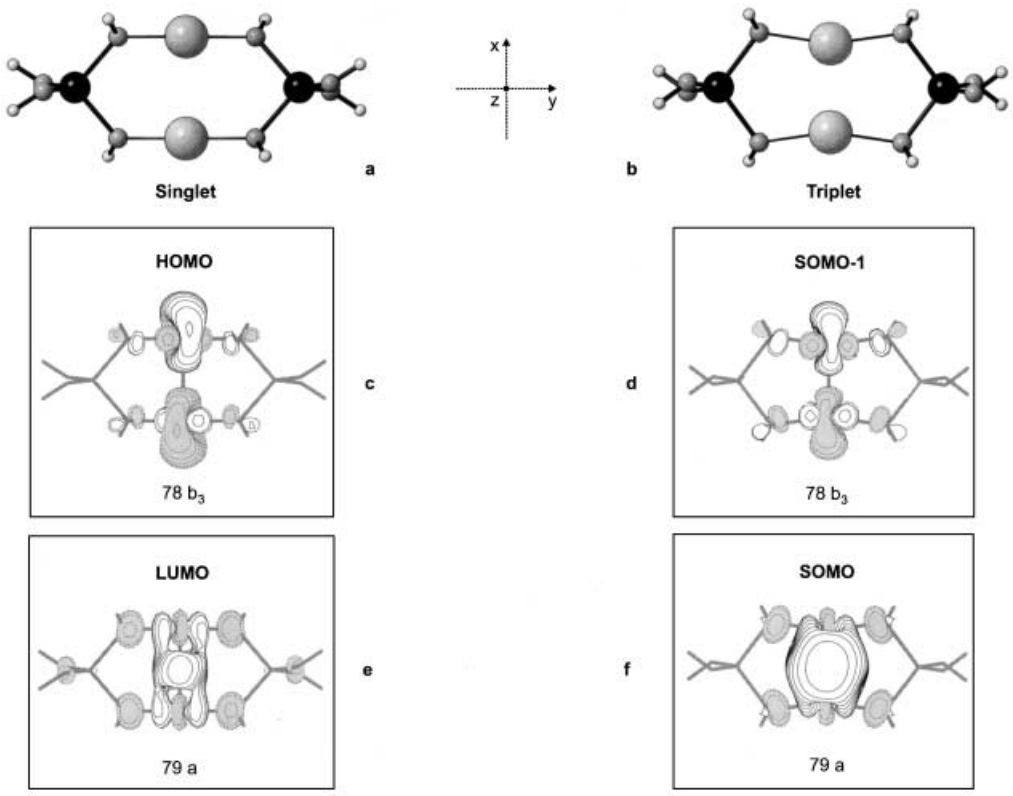

Figure 12. a) Optimized D_2-[{CuAl(OH)$_4$}$_2$] model in the electronic ground state (^{1}A). b) Optimized D_2-[{CuAl(OH)$_4$}$_2$] model in the first excited electronic state (^{3}B$_3$). c) HOMO of the ^{1}A state with b_3 symmetry. d) Second-highest SOMO from ROB3LYP calculations of the first excited electronic state (^{3}B$_3$) with b_3 symmetry, which corresponds to the HOMO of the electronic ground state. e) LUMO of the ^{1}A state with a symmetry. f) Highest SOMO from ROB3LYP calculations of the first excited electronic state (^{3}B$_3$) with a symmetry, which corresponds to the LUMO of the electronic ground state. Molecular orbitals have been depicted with the aid of the program Molden.[50]

  0947-6539/02/0809-2110 $ 20.00+.50/0 *Chem. Eur. J.* **2002**, *8*, No. 9

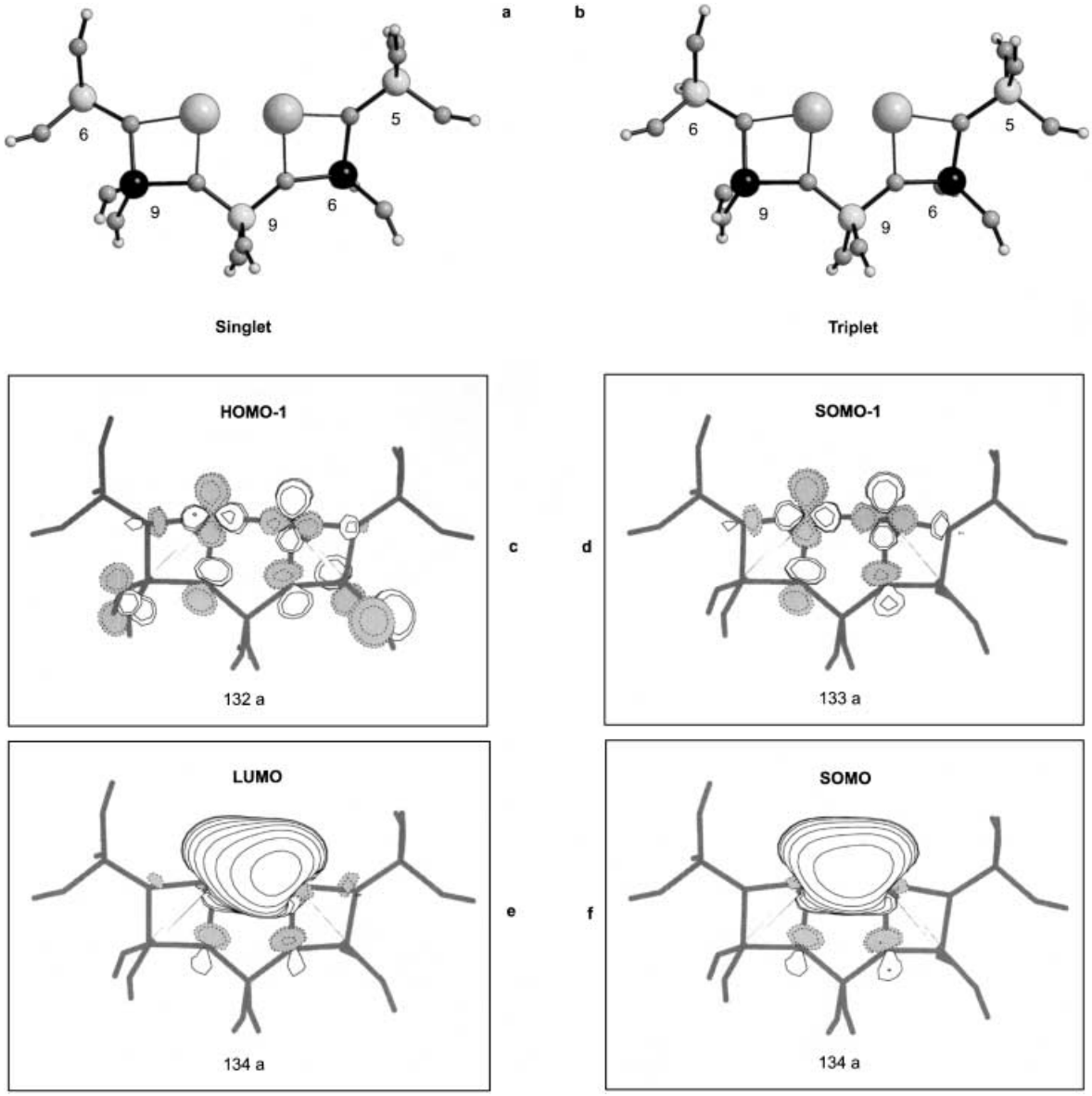

Figure 13. a) C_1-symmetric QM-Pot structure of the ***O***(6,9/1) pair in its electronic ground state (^{1}A). b) C_1-symmetric QM-Pot structure of the ***O***(6,9/1) pair in its first excited electronic state (^{3}A). c) Second-highest occupied MO of the ^{1}A state. d) Second-highest SOMO from ROB3LYP calculations of the first excited electronic state (^{3}A) which corresponds to the second-highest occupied MO of the ^{1}A state. e) LUMO of the ^{1}A state. f) Highest SOMO from ROB3LYP calculations of the first excited electronic state of the (^{3}A) which corresponds to the LUMO of the ^{1}A state.

linearly combined to an MO with antibonding character. In the SOMO the linear combination of these atomic hybrid orbitals leads to an MO of bonding character, fully in line with the situation for the D_2-[{CuAl(OH)$_4$}$_2$] model above. Accordingly, the Cu[I]–Cu[I] distance is shortened by 0.22 Å upon single occupation of the SOMO in the triplet state. The NBO analysis assigns slight differences to the electronic structure of the singlet states of both systems:[49] atomic 3d–4s hybridization of Cu[I] is slightly less pronounced in the ***O***(6,9/1) system, with a $3d^{9.84}4s^{0.25}$ population, than in the D_2-[{CuAl(OH)$_4$}$_2$] model ($3d^{9.73}4s^{0.48}$). In the triplet state, however, the occupation pattern is very similar ($3d^{9.51}4s^{0.66}$ vs. $3d^{9.45}4s^{0.72}$, see Table 8).

Table 8. Results of NBO analysis for the ***O***(6,9/1) model system with RB3LYP and ROB3LYP, respectively. Average values are given.

	Natural charges			Natural population				
Atom	Singlet	Triplet	Orbital	Singlet	Triplet total	Triplet α	Triplet β	Spin density[a]
Cu	0.88	0.79	4s	0.25	0.66	0.51	0.15	0.87
			3d	9.84	9.51	4.98	4.51	
O[b]	– 1.43	– 1.41	2s	1.80	1.80	0.9	0.9	0.06
			2p	5.63	5.61	2.84	2.78	
Al	2.17	2.17						
Si	2.57	2.58						

[a] Mulliken analysis. [b] Oxygen atoms next to the copper atoms.

  0947-6539/02/0809-2111 $ 20.00+.50/0

Energetically, the first excited electronic state ($^3B_3$) of the D_2-[{CuAl(OH)$_4$}$_2$] model is 3.0 eV higher than the singlet ground state (see Table 9) and the vertical transition energies are computed as 2.6 eV and 3.4 eV for the $S_0 \leftarrow T_1$ and the $T_1 \leftarrow S_0$ process in the D_2-[{CuAl(OH)$_4$}$_2$] model. For the QM-Pot results on the larger systems we generally note much smaller singlet – triplet gaps (Table 9) and they cover a broad range from 0.9 – 3.2 eV (excitation) and 0.3 – 1.7 eV (emission).

Table 9. Excitation and emission energies [eV].

Classification	$E(T_1 \leftarrow S_0)$	$E(S_0 \leftarrow T_1)$	$E(T_1) - E(S_0)$	r(Cu – Cu)[a]
D_2-[{CuAl(OH)$_4$}$_2$]	3.41	2.58	2.97	2.37
N′[b] // ***N1***(7′,10′/1)	3.08	2.07	3.43	2.36
N1(7′,10′/1)	3.10	1.68	2.29	2.36
N1(1,7/2)	2.91	0.95	1.70	2.46
N1(4,10/2)	2.66	0.56	1.45	2.69
O(2,12/1)	0.90	0.32	0.49	2.37
O(6,9/1)	0.72	0.25	0.40	2.33
O(2,5/1)	0.71	0.31	0.46	2.38
N2(7,12/2)	2.00	0.78	1.12	2.37
N2(7,12/1)	1.51	0.77	1.03	2.35
N3(9,10/1)	1.61	0.69	1.04	2.37
C(5,11/2)[c]	3.21			
ON(7,12/2)	1.77	0.88	1.18	2.36

[a] Cu – Cu distance [Å] for the structure in the triplet state. [b] Small model system of ***N1***(7′,10′/1) with fixed O–H bond lengths and a structure as obtained by QM-Pot calculations for the model system of regular cluster size. [c] In the triplet state the Cu^I ions separate and one Cu^I ion is migrating into the sinusoidal channel. Thus the triplet does not have the characteristic of a cage pair and is not considered here.

The noticeable differences between transition energies for the D_2-[{CuAl(OH)$_4$}$_2$] model and the ***N1***(7′,10′/1) pair are caused by differences in the structure of the local environment, as demonstrated by calculations on a smaller model for the ***N1***(7′,10′/1) pair, denoted as ***N′*** (see Figure 14c and d). Atomic positions were taken from the QM-Pot structures of the standard models (Figure 14a and b) and the O–H bonds were kept frozen. The transition energies for this system agree with the QM-Pot results for the ***N1***(7′,10′/1) pair for the vertical $T_1 \leftarrow S_0$ transition but not with those for the vertical $S_0 \leftarrow T_1$ nor with those for the adiabatic energy difference. This discrepancy is clearly caused by the neglect of two coordinating oxygen atoms present in the larger system in the triplet state.

Evidently, the local environment of the Cu^I ions has a significant influence on the transition energies. While this does not come as a surprise, it can be illustrated best by comparing singlet – triplet energy gaps for smaller model systems of identical constitution, ***O′*** and ***N′***, representing the larger ***O***(6,9/1) and ***N1***(7′,10′/1) sites considered above. The structures of these two systems were taken from the QM-Pot results of the regular larger clusters optimized for the singlet and triplet states (Figure 15). O–H bond lengths were optimized while all atomic positions except for those of the hydrogen atoms were kept frozen. From comparison of the

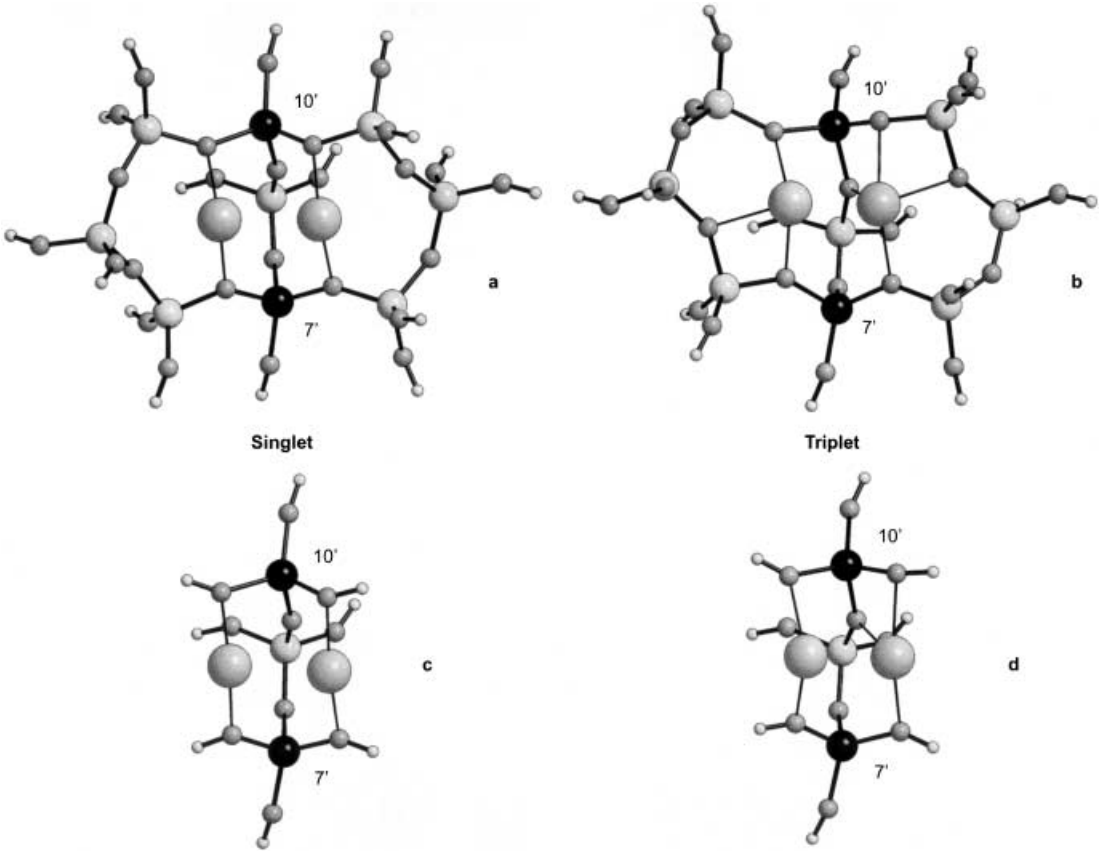

Figure 14. a) Model system of the ***N1***(7′,10′/1) pair in its electronic ground state (^{1}A). b) Model system of the ***N1***(7′,10′/1) pair in the first excited electronic state (^{3}A). c) Model system ***N′*** in its electronic ground state (^{1}A) with the structure of (a). d) Model system ***N′*** in the the first excited electronic state (^{3}A) with the structure of (b).

  0947-6539/02/0809-2112 $ 20.00+.50/0 *Chem. Eur. J.* **2002**, *8*, No. 9

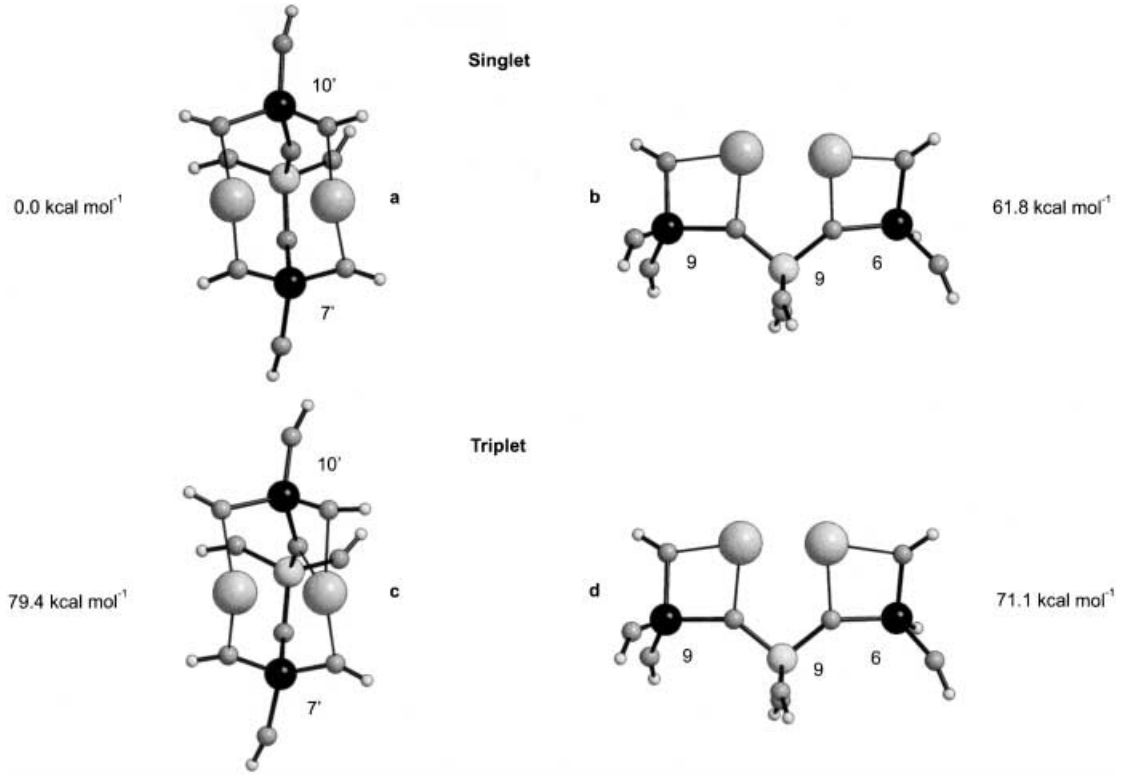

Figure 15. a) Model system ***N′*** in its electronic ground state (^{1}A). b) Model system ***O′*** in its electronic ground state (^{1}A). c) Model system ***N′*** in its first excited electronic state (^{3}A). d) Model system ***O′*** in its first excited electronic state (^{3}A). Energies given are relative to ***N′*** in its electronic ground state (^{1}A).

energies computed for ***O′*** and ***N′*** we see that the singlet state of ***N′*** is 62 kcal mol^{-1} more stable than singlet ***O′***. Triplet ***O′***, however, is found to be 8 kcal mol^{-1} more stable than triplet ***N′***. Thus, the larger singlet–triplet gap computed for the nest pair (79 kcal mol^{-1} or 3.4 eV) compared with the open site (9 kcal mol^{-1} or 0.4 eV) results from the high stability of the singlet ground state species while the triplet spin state is of similar energy. It is thus the particular linear oxygen coordination mode of the two copper ions within the nest structures that render this species special in terms of excitation and emission spectroscopic properties. We note in passing that the even higher $T_1 \leftarrow S_0$ gap computed for the ***C***(5,11/2) site is due to a highly unstable triplet state: geometry optimization of the triplet state species leads to dissociation of the two copper ions.

None of our computed excitation or emission energies provides an unambiguous explanation for experimental data: bands in the photoluminescence spectra have been reported at 490 nm (2.53 eV) and 535 nm (2.32 eV) (Lamberti et al.),[11] at 480 nm (2.58 eV) and 540 nm (2.30 eV) (Wichterlová et al.),[15, 19, 20] or at 420 nm (2.95 eV), 470 nm (2.64 eV), and 520 nm (2.38 eV) (Anpo et al.)[21]. The observed bands in the excitation spectra are at 256 nm (4.84 eV) and 300 nm (4.13) (Lamberti et al.)[11] and at 310 nm (4.00 eV) (Anpo et al.).[21] On the basis of the present results we cannot assign any of the experimentally observed bands to Cu[I] pairs even if we take into consideration the fact that our calculated excitation energies are systematically too low (we have calculated energies for $T_1 \leftarrow S_0$ transitions instead of $S_1 \leftarrow S_0$ transitions observed experimentally). We would not expect the occurrence of distinct bands anyway, because of the scant Cu contents present in the Cu-ZSM-5 samples used for the spectroscopic measurements (two copper ions per unit cell at most) and the necessity of Al atoms at appropriate framework positions. Cu[I] pairs, if present at all, would thus represent only a small fraction of the total population of Cu species. The occurrence of isolated Cu[I] sites is more likely. On the basis of our results we feel it is safe to rule out earlier suggestions that the 520 nm emission band observed in the photoluminescence spectra is due to Cu[I] pairs.[21] A computational study on photoluminescence spectra instead suggests that the bands observed correspond to two different types of isolated Cu[I] sites.[17]

Conclusions

Notwithstanding their formal charge and closed shell d^{10} electronic configuration, Cu[I] ions can form pairs in Cu-ZSM-5 provided Al atoms are present at appropriate framework positions. By means of a state-of-the-art quantum chemical/interatomic potential function approach, we have located various types of possible Cu[I] pairs, which we classified as *open*, *nest*, *open-nest*, and *cage* pairs. Open pairs are located at chain-shaped sites at the intersection of the main and the sinusoidal channel. Nest pairs were found in the sinusoidal channel. The group of nest pair sites consists of bridged seven- and eight-membered rings. Open-nest pairs were found in the main channel. Cage pairs are located in an area that belongs neither to the main nor to the sinusoidal channel.

The majority of pairs are energetically slightly less stable than separated monomers. Taking entropic effects into consideration further disfavors pairs. However, the nest 1 coor-

  0947-6539/02/0809-2113 $ 20.00+.50/0

dination site constitutes an exceptional species, which is the most stable coordination site for Cu^I pairs. It consists of an eight-membered ring bridged by one T site and is found for many different Al distributions. Most ***N1*** pairs show a parallel arrangement of two linear O-Cu^I-O units. In particular we found that ***N1***(7′,10′/1), in which two linear O-Cu^I-O units are located between two Al sites, was energetically favored over all other pairs or monomers. However, this site can exist only if Al atoms are present in next-nearest-neighbor T7 and T10 positions.

Calculated vertical singlet–triplet transition energies for both singlet- and triplet-optimized pair structures give evidence that no distinct Cu^I pair band in the excitation and emission spectra can be expected. The assignment of the emission band at 520 nm to Cu^I pairs cannot be supported. Our calculations confirm the conclusion of a previous study that the observed photoluminescence bands are due to isolated Cu^I sites.[17]

On the basis of our results we propose the following minimum requirements for zeolites in which there could be a significant population of Cu^I pairs: the material must contain eight-membered rings bridged by one T site (two six-membered rings sharing three T sites). The Si/Al ratio must be low and the Cu^I loading high. For the preparation procedure, a direct Cu^I ion exchange should be favored over Cu^{II} ion exchange followed by a reduction, in order to avoid the blocking of possible pair coordination sites by Cu^{II} ions. If Cu^{II} ions are used in the preparation phase, however, repeated exchange and reduction steps seem necessary. Samples prepared in this way could possibly contain some pairs and allow for further investigation of the catalytic role of Cu^I pairs in the deNO_x process.

By analogy with bioinorganic approaches to model enzymatic catalysis by investigation of *biomimetic* model systems, we believe that the experimental investigation of *zeomimetic* models of possible active sites in zeolites could be a promising approach for the study of their reactivity. With respect to the present results, it would be interesting to investigate model systems mimicking the ***N1***(7′,10′/1) pair.

Acknowledgements

MCH gratefully acknowledges financial support from the Fonds der Chemischen Industrie through a Liebig-Stipendium. This work has been supported by the Deutsche Forschungsgemeinschaft, the Max Planck Society, the Fonds der Chemischen Industrie and the Max-Buchner-Forschungsstiftung. Computer time and excellent service (Dr. Thomas Steinke) was provided by the Konrad Zuse Zentrum für Informationstechnik Berlin (ZIB). We thank Dr. Marek Sierka for helpful discussions.

[1] M. Iwamoto, H. Furukawa, Y. Mine, F. Uemura, S. Mikuriya, S. Kagawa, *J. Chem. Soc. Chem. Commun.* **1986**, 1272.
[2] M. Shelef, *Chem. Rev.* **1995**, *95*, 209.
[3] G. Spoto, S. Bordiga, D. Scarano, A. Zecchina, *Catal. Lett.* **1992**, *13*, 39.
[4] Y. Chang, J. G. McCarty, *J. Catal.* **1997**, *165*, 1.
[5] J. Varga, J. Halàsz, I. Kiricsi, *Environ. Pollut.* **1998**, *102*, 691.
[6] W. F. Schneider, K. C. Hass, R. Ramprasad, J. B. Adams, *J. Phys. Chem. B* **1998**, *102*, 3692.
[7] H. van Koningsveld, J. C. Jansen, H. van Bekkum, *Zeolites* **1990**, *10*, 235.
[8] S. C. Larsen, A. Aylor, A. T. Bell, J. A. Reimer, *J. Phys. Chem.* ***1994***, *98*, 11533.
[9] W. Grünert, N. W. Hayes, R. W. Joyner, E. S. Shpiro, M. R. H. Siddiqui, G. N. Baeva, *J. Phys. Chem.* **1994**, *98*, 10832.
[10] T. Beutel, J. Sarkany, G.-D. Lei, J. Y. Yan, W. M. H. Sachtler, *J. Phys. Chem.* **1996**, *100*, 845.
[11] C. Lamberti, S. Bordiga, M. Salvalaggio, G. Spoto, A. Zecchina, *J. Phys. Chem. B* **1997**, *101*, 344.
[12] G. Moretti, *Catal. Lett.* **1994**, *23*, 135.
[13] G. Moretti, *Catal. Lett.* **1994**, *28*, 143.
[14] G. Moretti, C. Dossi, A. Fussi, S. Recchia, R. Psaro, *Appl. Catal. B* **1999**, *20*, 67.
[15] B. Wichterlová, J. Dědeček, Z. Sobalík, A. Vondrová, K. Klier, *J. Catal.* **1997**, *169*, 194.
[16] M. Iwamoto, H. Yahiro, K. Tanda, N. Mizuno, Y. Mine, S. Kagawa, *J. Phys. Chem.* **1991**, *95*, 3727.
[17] D. Nachtigallová, P. Nachtigall, M. Sierka, J. Sauer, *Phys. Chem. Chem. Phys.* **1999**, *1*, 2019.
[18] P. Nachtigall, D. Nachtigallová, J. Sauer, *J. Phys. Chem. B* **2000**, *104*, 1738.
[19] J. Dědeček, B. Wichterlová, *J. Phys. Chem.* **1994**, *98*, 5721.
[20] B. Wichterlová, J. Dědeček, A. Vondrová, *J. Phys. Chem.* **1995**, *99*, 1065.
[21] M. Anpo, M. Matsuoka, Y. Shioya, H. Yamashita, E. Giamello, C. Morterra, M. Che, H. H. Patterson, S. Webber, S. Ouellette, M. A. Fox, *J. Phys. Chem.* **1994**, *98*, 5744.
[22] H. Yamashita, M. Matsuoka, K. Tsuji, Y. Shioya, M. Anpo, M. Che, *J. Phys. Chem.* **1996**, *100*, 397.
[23] Y.-J. Huang, H. Paul Wang, J.-F. Lee, *Chemosphere* **1999**, *39*, 1347.
[24] H. Hamada, N. Matsubayashi, H. Shimada, Y. Kintaichi, T. Ito, A. Nichijima, *Catal. Lett.* **1990**, *5*, 189.
[25] J. Sauer, M. Sierka, *J. Comp. Chem.* **2000**, *21*, 1470.
[26] U. Eichler, C. M. Kölmel, J. Sauer, *J. Comput. Chem.* **1997**, *18*, 463.
[27] M. Sierka, J. Sauer, *J. Chem. Phys.* **2000**, *112*, 1.
[28] P. Nachtigall, D. Nachtigallová, J. Sauer, *Phys. Chem. Chem. Phys.* **2001**, *3*, 1552.
[29] "Catalysis by Unique Metal Ion Structures in Solid Matrices": J. Sauer, D. Nachtigallová, P. Nachtigall, *NATO Sci. Ser. II* **2001**, *13*, 221.
[30] L. Rodriguez-Santiago, M. Sierka, V. Branchadell, M. Sodupe, J. Sauer, *J. Am. Chem. Soc.* **1998**, *120*, 1545.
[31] P. Nachtigall, M. Davidová, D. Nachtigallová, *J. Phys. Chem. B* **2001**, *105*, 3510.
[32] K. Teraishi, M. Ishida, J. Irisawa, M. Kume, Y. Takahashi, T. Nakano, H. Nakamura, A. Miyamoto, *J. Phys. Chem. B* **1997**, *101*, 8079.
[33] D. C. Sayle, C. R. A. Catlow, M.-A. Perrin, P. Nortier, *Microporous Mesoporous Mater.* **1998**, *20*, 259.
[34] B. R. Goodman, K. C. Hass, W. F. Schneider, J. B. Adams, *J. Phys. Chem. B* **1999**, *103*, 10452.
[35] a) R. Ahlrichs, M. Bär, M. Häser, H. Horn, C. Kölmel, *Chem. Phys. Lett.* **1989**, *162*, 165; b) O. Treutler, R. Ahlrichs, *J. Chem. Phys.* **1995**, *102*, 346.
[36] J. D. Gale, *J. Chem. Soc. Faraday Trans.* **1997**, *93*, 629.
[37] *Gaussian 98* (Revision A.7), M. J. Frisch, G. W. Trucks, H. B. Schlegel, G. E. Scuseria, M. A. Robb, J. R. Cheeseman, V. G. Zakrzewski, J. A. Montgomery, R. E. Stratmann, J. C. Burant, S. Dapprich, J. M. Millam, A. D. Daniels, K. N. Kudin, M. C. Strain, O. Farkas, J. Tomasi, V. Barone, M. Cossi, R. Cammi, B. Mennucci, C. Pomelli, C. Adamo, S. Clifford, J. Ochterski, G. A. Petersson, P. Y. Ayala, Q. Cui, K. Morokuma, D. K. Malick, A. D. Rabuck, K. Raghavachari, J. B. Foresman, J. Cioslowski, J. V. Ortiz, B. B. Stefanov, G. Liu, A. Liashenko, P. Piskorz, I. Komaromi, R. Gomperts, R. L. Martin, D. J. Fox, T. Keith, M. A. Al-Laham, C. Y. Peng, A. Nanayakkara, C. Gonzalez, M. Challacombe, P. M. W. Gill, B. G. Johnson, W. Chen, M. W. Wong, J. L. Andres, M. Head-Gordon, E. S. Replogle, J. A. Pople, Gaussian, Inc. (Pittsburgh, PA), **1998**.
[38] W. Koch, M. C. Holthausen, *A Chemist's Guide to Density Functional Theory, 2nd ed.*, Wiley-VCH, Weinheim, **2001**.
[39] A. D. Becke, *J. Chem. Phys.* **1993**, *98*, 5648.
[40] A. Schäfer, H. Horn, R. Ahlrichs, *J. Chem. Phys.* **1992**, *97*, 2571.
[41] K.-P. Schröder, J. Sauer, *J. Phys. Chem.* **1996**, *100*, 11043.
[42] M. Sierka, J. Sauer, *Faraday Discuss.* **1997**, *106*, 41.
[43] P. Pykkö, *Chem. Rev.* **1997**, *97*, 597.

  0947-6539/02/0809-2114 $ 20.00+.50/0

[44] F. A. Cotton, G. Wilkinson, *Advanced Inorganic Chemistry, 4th ed.*, Wiley, New York, **1980**.
[45] K. Iijima, T. Itoh, S. Shibata, *J. Chem. Soc. Dalton Trans.* **1985**, 2555.
[46] U. Eichler, M. Brändle, J. Sauer, *J. Phys. Chem. B* **1997**, *101*, 10035 and references cited therein.
[47] E. Dempsey, G. H. Kühl, D. H. Olson, *J. Phys. Chem.* **1969**, *73*, 387.
[48] K.-P. Schröder, J. Sauer, *J. Phys. Chem.* **1993**, *97*, 6579.
[49] Modification of the Gaussian 98 source code (link 607) was necessary in order to allow NBO analyses for systems with more than 500 contracted basis functions.
[50] G. Schaftenaar, J. H. Noordik, "Molden: a pre- and post-processing program for molecular and electronic structures", *J. Comput.-Aided Mol. Design* **2000**, *14*, 123.

Received: July 30, 2001 [F3459]

  0947-6539/02/0809-2115 $ 20.00+.50/0